CHARACTERIZATION OF THE ADHESION OF CALCIUM OXALATE MONOHYDRATE CRYSTALS ON PHOSPHOLIPID MEMBRANES BY ELLIPSOMETRY

By

ANNE-SOPHIE WIDEDE BOURIDAH

A THESIS PRESENTED TO THE GRADUATE SCHOOL
OF THE UNIVERSITY OF FLORIDA IN PARTIAL FULFILLMENT
OF THE REQUIREMENTS FOR THE DEGREE OF
MASTER OF SCIENCE

UNIVERSITY OF FLORIDA

2008

To my dad, the person I admire the most and my mom, the most wonderful woman.

ACKNOWLEDGMENTS

I would like to thank Dr. Daniel R. Talham for giving me the opportunity to work in his group and providing such a great learning experience. I would like to acknowledge all the members of the Talham group, especially Roxane Fabre for our collaboration on the ellipsometer instrument, Monique Williams for making the lab a joyful place to be, Denise Sharbaugh for helping me in the COM project. Also deserving thanks are Ian Rummel and Justin Gardner for their constant help in the lab.

My acknowledgements also go to Dr. Ben Smith for giving me the wonderful opportunity to join the Department of Chemistry of the University of Florida and Lori Clark for helping in every steps of the integration.

Finally, I want to particularly thank my parents, Karim and Marie-Paule Bouridah, for all their love, constant encouragement and support. I am and will always be indebted to them for making everything I have accomplished possible, for believing in me and giving me the best moral support in every single day. My sister, Maud Bouridah, deserves a special mention. She always knows how to cheer me up and make me smile in the toughest times. Also deserving of thanks are my grandmother, grandaunt and the rest of my family who always believed in me. Finally, I would like to give special recognition to my friends who stayed close to my heart even oceans apart.

TABLE OF CONTENTS

page

LIST OF TABLES

LIST OF FIGURES

Abstract of Thesis Presented to the Graduate School
of the University of Florida in Partial Fulfillment of the
Requirements for the Degree of Master of Science

CHARACTERIZATION OF THE ADHESION OF CALCIUM OXALATE MONOHYDRATE CRYSTALS ON PHOSPHOLIPID MEMBRANES BY ELLIPSOMETRY

By

Anne-Sophie W. Bouridah

December 2008

Chair: Daniel R. Talham
Major: Chemistry

Calcium oxalate monohydrate (COM) is one the most common inorganic components found in kidney and urinary tract stones. Stones are found attached to the tip of renal papilla, through adhesive contacts. In vitro studies suggested that anionic molecules such as phospholipids may serve as adhesives that promote calcium oxalate monohydrate crystals attachment to epithelial cells.

Ellipsometry and SPR enhanced ellipsometry are nonperturbative and quantitative methods and allow large-area measurements of small optical changes. In this study these methods are used to characterize the crystal-lipid interactions. Using imaging ellipsometry and kinetic analysis, the formation of phospholipid monolayer and bilayers is observed, surface coverage, lateral uniformity and film thickness are characterized. Real-time measurements by ellipsometry and SPR enhanced ellipsometry allowed the interaction of COM crystals with different phospholipid to be characterized, and demonstrate the adhesion of COM crystals on POPC while DMPC is not subjected to such phenomenon.

CHAPTER 1
INTRODUCTION

Background

Kidney stones affect 12% of men and 4% of women in the American population. They can be extremely painful and expensive to treat. 50% of people treated for a kidney stone will have a recurrence within 10 years. Stones can be deposits of calcium phosphates, uric acid, struvite, or even calcium carbonate, but most common have calcium oxalate as their main component, usually in its monohydrate form.[1] The inorganic crystals are mixed with an organic matrix composed of proteins, carbohydrates, lipids, and other cellular components that account for about 2 to 3% of the total mass of the stones, although a much larger percentage of the total volume.

Studies show that urinary concentrations and the rate of fluid flow in the kidney provide insufficient transit time for crystals to grow large enough to be occluded and retained. However, in some cases, the crystals remain inside the kidneys and initiate the process of stone formation. Crystal attachment to the kidney's tubular cell surface is therefore a critical step in pathological calcification.

Tissue culture studies have provided insights into renal responses to calcium oxalate exposure. LLC-PK1 cells are commonly used to represent the proximal tubular cells and MDCK cells to represent epithelial cells of the more distal sections of the renal tubules. Epithelial injury has been shown to promote attachment of calcium oxalate crystals.[1] Tissue injury can cause loss of membrane lipid asymmetry or cell polarity leading to changes in the composition and physical properties of the plasma membrane that alter crystal-membrane interactions. Stones often are found attached to the tip of renal papilla, through adhesive contacts.[2] In vitro studies have suggested that anionic molecules and urinary proteins with substantial anionic functionalities

may serve as adhesives that promote calcium oxalate monohydrate crystals (COM) aggregation and attachment to epithelial cells. Anionic molecules such as phospholipids which are embedded in epithelial cell membranes, are also thought to promote the attachment of COM to renal tubules.[3] Acidic phospholipids, lipid extracts from calcified crystals, membranes of matrix vesicles, and liposomes have all been shown to initiate calcium phosphate precipitation *in vitro* in metastable solutions. However, certain urinary molecules are thought by others to suppress crystal aggregation and cell attachment, presumably because of adsorption on COM crystal faces. [4]

Sheng et al. measured the adhesion forces between functional groups immobilized on the tip of an atomic-force microscope (AFM) and prominent COM crystal faces.[5] In this configuration, an AFM tip modified with certain functional groups could be viewed as a mimic of urinary protein segments or crystal-recognition sites embedded in epithelial cell membranes. Tip-immobilized carboxylate and amidinium groups displayed the largest adhesion forces, and adhesion is sensitive to the structure and composition of crystal faces.[5]

Sandersius and Rez investigated the morphology of calcium oxalate crystals with atomic force microscopy (AFM) and scanning electron microscopy (SEM).[6] Images obtained after proteolysis show that the crystals are in the form of plates stacked on (100) surfaces. This face has been documented in studies involving membrane adhesion and COM precipitation in cell cultures rich in lipids. The (100) face is calcium-rich and slightly positive; two of the typical Ca^{2+} coordination sites are vacant. Lipid head groups that can bind calcium will stabilize this face and allow for its expression.

Rabinovich et al. also studied AFM interaction forces between COM crystal colloidal probes and monolayers of renal epithelial cells in artificial urine solutions. The adhesion force

was measured for the COM/MDCK cell interaction, while no adhesion force was found for the COM/LLC-PK1 cell interaction. The adhesion difference between LLC-PK1 and MDCK cells possibly explains the preferential deposition of crystals only in collecting ducts (lined with MDCK-type cells) and the lack of the crystal deposition in the proximal tubules (lined with LLC-PK1-type cells).[7] Atomic force microscopy is amenable to a broader range of substrate but suffer from tip-induced perturbations.

To better understand the process of stone formation, it is important to study interactions between the organic and crystalline components. Our group has previously performed a series of studies on calcium oxalate precipitation at an interface provided by phospholipid Langmuir monolayers that serve as models for the phospholipid domains within membranes.[8] Langmuir monolayers, in general, are comprised of molecules that contain both hydrophobic and hydrophilic regions and are traditionally formed at the air-water interface. Previous work has demonstrated the ability of phospholipids to induce nucleation of COM at Langmuir monolayers at the air-water interface.[27] Studies have been done to elucidate the nature of this interaction by varying the lipids, the polar head groups and alkyl tails, the surface pressure and phases, temperature, and composition, such as adding sphingolipids and cholesterol.[29, 30, 33] Evidence has been presented that phase boundaries within the lipid matrix have a profound effect on nucleation and crystallization.[34] However, work at the air-water interface is considerably constrained.

Brewster angle microscopy images illustrate various regions and conditions that can promote COM growth at a phase boundary, but this particular optical technique, although robust, has distinct limitations. The region of a monolayer that is viewable is small and COM crystals are not visible immediately following nucleation due to optical constraints.

In order to extract further information about the interaction between phospholipids and COM, other ways to examine this interaction requires transferring lipid monolayers to a solid substrate. Monolayers and bilayers can be transferred to a solid substrate and generated through vesicle adsorption and rupture. This method creates an easily reproducible bilayer that, once characterized, can be subjected to COM seed crystals solution. By using a lipid vesicle adsorption and rupture method, many of the inherent problems with phospholipids transfer are eliminated.

Through the use of ellipsometry and surface plasmon resonance (SPR) enhanced ellipsometry, the monitoring of bilayer formation can be observed followed by the adhesion of COM seed crystals on the phospholipid bilayer both *in situ* and *ex situ*. From the vantage of supported membrane research, ellipsometry offers a nonperturbative, quantitative method and allows *in situ*, label-free, spatially resolved, and large-area measurements of small spatial or temporal differences in the optical functions following bilayer depositions with reasonably short collection time determined by the video rate of the CCD detector. The *ex situ* characterization of the crystals-lipids interaction by surface plasmon resonance, not yet reported in literature, may provide new information about the interaction, namely the kinetics of the adhesion, quantification, and surface coverage.

Ellipsometry

Ellipsometry, widely used for surface and thin-film analysis, is a very sensitive, non-destructive experimental technique. In the most general terms, it is based on polarization changes that occur on the reflection of a polarized monochromatic light at an oblique incidence (Figure 1-1).[9] The basic quantity measured in an ellipsometric experiment is the complex reflectance ratio:

$$\rho = \frac{\chi_r}{\chi_i} \qquad (1)$$

where χ_r and χ_i represent the state of polarization of the reflected and incident beams, respectively. For samples that can be approximated by isotropic optical functions or scale refractive indices, Eq.1 is written as below:

$$\rho = \frac{R_p}{R_s} = \tan(\psi) * e^{i\Delta} \qquad (2)$$

where R_p and R_s are the complex reflection coefficients for the light polarized parallel and perpendicular to the plane of incidence, respectively. In this method, the polarizer (p) and analyzer (a) angles can be related to the measured parameters by the following equations:

$$\Delta = 2p + \frac{\pi}{2} \qquad (3) \qquad\qquad \psi = |a| \qquad (4)$$

Ellipsometry is an indirect technique, and extracting relevant physical information about the sample requires the use of optical models typically based on classical electromagnetic theory and the approximation of the sample in terms of parallel optical slabs of defined thicknesses (d) and refractive indices (n+ik). The quantitative accuracy of the physical properties determined directly depends on how faithfully the slab model depicts the optical properties of the actual experimental sample.[9] Ellipsometry offers a nonperturbative, quantitative method for large-area measurements of small spatial or temporal difference in the optical functions for kinetics analysis.

Surface Plasmon Resonance

The SPR phenomenon has been discovered in the early 20th century and occurs on the conditions of total internal reflection by thin layers of noble metals like gold, silver and copper. The surface selectivity of SPR comes from the excitation of surface plasmon polaritons at the metal-dielectric interface. Those plasmons are electromagnetic modes that represent a coupled state between oscillations of the electron plasma in the metal with high frequency

electromagnetic fields. They propagate along the surface with amplitude decaying exponentially in the direction perpendicular to the interface and can interact with molecules close to the interface (Figure 1-2). Adsorption or desorption of molecules change the refractive index in the interfacial region, thus will shift the resonance angle (Figure 1-3). The Kretschmann configuration is used to create the evanescent field on the gold surface, where the polarized light is directed through the prism with a high refractive index (n=1.72) to the thin layer of gold in contact with the buffer solution with a low refractive index (n=1.33).

Typical SPR experiments measure the energy reflectance R_p of p-polarized light at a fixed wavelength as a function of the incidence angle. At angles of incidence higher than the critical angle, the light is totally reflected back into the prism. There exists a specific angle of incidence where the x-component of the k-vector of the evanescent field matches the wave vector of the plasmon oscillations at the metal/dielectric interface. The energy will be transferred to the surface plasmons of the gold layer that generated resonance plasmons and causes a reduction in the intensity if the reflected light. The observed minimum depends on different parameters of the reflecting system, which are the refractive index (n), the extinction coefficient (k) and the thickness (d) of the different layers.

Surface Plasmon Resonance enhanced Ellipsometry

Recently, the possibility of using the change in the phase of the reflected light through the SPR minimum to determine the refractive index of the medium has been investigated.[10] This phase change is far more rapid than the change in reflectivity, leading to a higher sensitivity. The first work which suggested the use of ellipsometry for surface Plasmon analysis appears to be in 1976 by Abeles.[11] Under SPR conditions, ellipsometric parameters give a large enhancement of detection sensitivity in comparison to SPR techniques. The advantage of coupling SPR with ellipsometry will allow us to observe the time for vesicles to deposit and lipid bilayer to form.

Real-time measurement of Δ and Ψ signal caused by the change on interface when phospholipids are subjected to COM crystals will also be accessible. Thus, it will be possible to follow and identify the interaction of calcium oxalate monohydrate crystals on the lipid bilayer without the laser having to go through the crystalline solution and be scattered.

In order to extract further information about these processes, the use of different techniques needs to be studied. Ellipsometry and SPR enhanced ellipsometry are nonperturbative and quantitative methods that allow large-area measurements of small optical changes. Monolayer and bilayer membranes can be formed by vesicle fusion onto a solid substrate. The first objective is to fabricate a solid-liquid cell adapted to the ellipsometer and to the study of lipid membrane interface.

After formation of large unilamellar vesicles, the purpose of this study is to characterize by Real-time measurements in situ and ex situ the deposition of monolayer and bilayer membranes by ellipsometry and SPR enhanced ellipsometry. Using imaging ellipsometry and kinetic analysis, two applications of the ellipsometry, the goal is to analyze the effect of the introduction of COM crystals, already prepared, on the supported phospholipid membranes. The aim of this study is to gather new information on the COM-lipid interaction with a new technique, never reported for the study of crystal-lipid interactions.

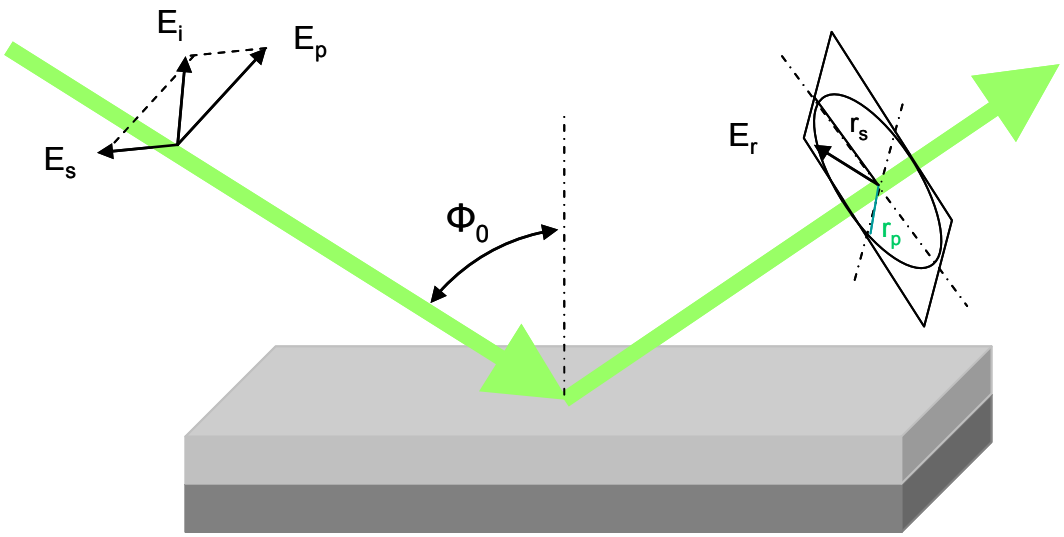

Figure 1-1. Ellipsometry measures the ratio of the reflection coefficients for the two components of the electromagnetic field-in the plane of incidence (p), and perpendicular (s). The increased sensitivity of ellisometry stems from the fact that the polarization-altering properties of the reflecting boundary are modified significantly even when ultrathin films are present.

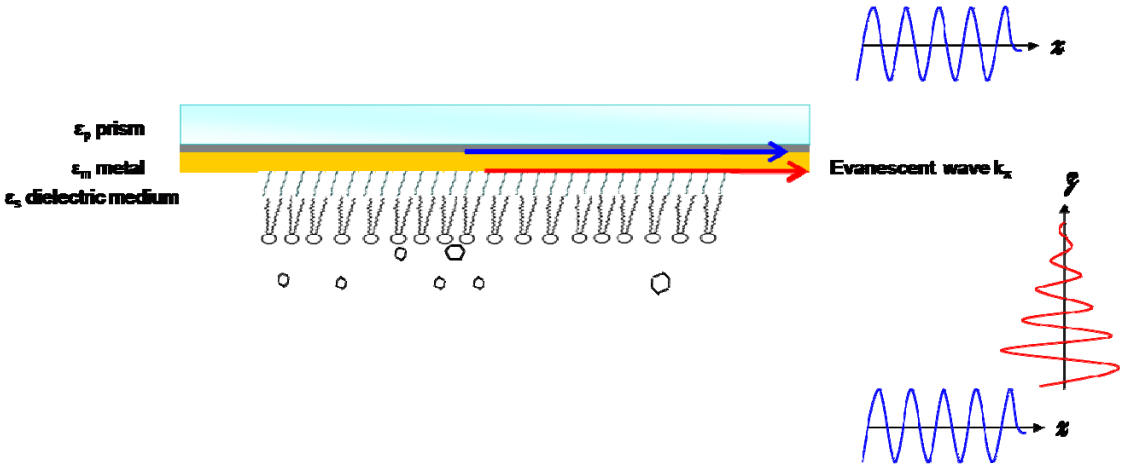

Figure 1-2. Light is directed through the substrate and the intensity of the resulting reflected light is measured with a detector. At certain incident light wavelengths and angles, part of the incident energy will couple into a surface plasmon wave traveling along the interface between the Au and the sample. This coupling is observed as a sharp attenuation in reflectivity and is known as the surface plasmon resonance effect. The angles and wavelengths where this effect is observed is extremely sensitive to the dieletric properties (or refractive index) of the sample in contact (~250 nm) with the metal surface

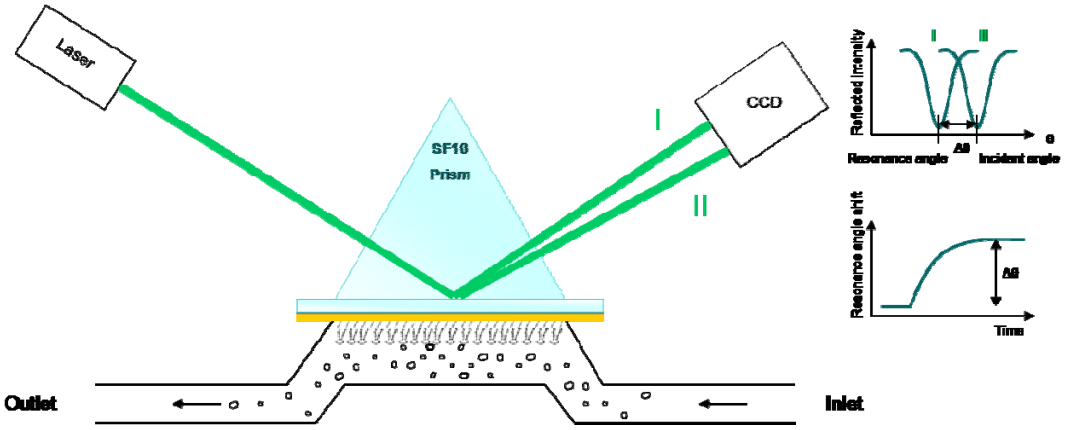

Figure 1-3. SPR enhanced ellipsometry principle. A change on the surface of the sensor chip is monitored by a change in refractive index close to the surface of the sensor chip.

CHAPTER 2
EXPERIMENTAL

Materials

Reagents were obtained from commercials sources. The 1,2-Dimyristoyl-sn-Glycero-3-Phosphocholine (DMPC) and 1-Palmitoyl-2-Oleoyl-sn-Glycero-3-Phosphocoline (POPC) monosodium were purchased from Avanti Polar Lipids (Alabaster, AL). All lipids were stored in a freezer (-20˚C) until use. Trizma Hydrochloride and Sodium Chloride were obtained from Sigma Co. (St Louis, MO). The refractive index matching fluid diiodomethane and octadecyl mercaptan were obtained from Sigma Aldrich (Milwaukee, WI). Calcium oxalate monohydrate crystals were purchased from Acros Organics (Morris Plains, NJ). Hydrogen peroxide (30% v/v) and sulfuric acid were purchased from Fisher Chemicals (Fairlawn, NJ) and used as received. All organic solvents were HPLC grade. All chemicals were used without further purification. Organic free deionized water of high resistivity (~ 17.9 MΩ-cm) was obtained from a reverse-osmosis deionization unit and coupled to a Millipore Synthesis water filtration unit (Barnstead). Trizma-buffered saline (TBS, 10 mM Trizma Hydrochloride and 100 mM NaCl, pH=7.4) was used as a vesicle spreading solution and buffer medium.

Solid-Liquid Cell

Fabrication of Solid-Liquid Cell for Ellipsometry

In order to characterize under aqueous conditions, a fluid cell had to be designed and used. This solid-liquid cell (SL cell) was specially designed for ellipsometric measurements on a non-transparent sample in liquid ambient. The shape and design was based on the solid-liquid cell of Nanofilm Technologie (Göttingen, Germany) in order to fit the EP^3-SW ellipsometer. This work was done in collaboration with Mr. Todd A. Prox, engineer and student machine shop supervisor of the Department of Chemistry of the University of Florida.

All schematics had to be prepared and drawn before proceeding to the fabrication of the cell (Figure 2-3 through 2-9). All materials of this cell were suited for use with aqueous solutions like salt solutions and buffers. Materials, dimensions and specifications are listed below:

- sample dimensions: 25 x 75 x 1 to 10 mm^3
- angle of incidence range: 58˚-63˚
- observable area at 60˚ angle of incidence(objective 10x): 38 x 54 mm^2
- material with liquid contact: PTFE® cover, Teflon® tubing (Valco Instruments, Co. Inc>, Schenkon, Switzerland), Viton® O-rings.
- liquid volume: 500µL
- windows: BK7 plan plates diameter: 10mm, thickness: 2mm (Edmund Optics, Barrington, NJ)
- standard HPLC fittings (OD. 1/16", ID. 0.02")
- O-rings, screws, syringes (5mL)

The liquid is injected into the cell by a peristaltic pump with a filling rate of about 0.4mL/min. Measurements of Δ and Ψ, the two ellipsometry parameters, are not affected by the cell, but the field of view and lateral resolution of the acquired images are limited by the objective and the CCD used. The specified accuracy in ellipsometric angle determination is 0.01˚ for our instrument.

Sample Preparation for Solid-Liquid Cell

Single-crystal silicon wafers (1 0 0) were obtained from International Silicon Solutions, Inc. (Dallas, TX) and cut to fit the Solid-Liquid Cell support (25mm x 15mm x 1mm). Before placing them in the Solid-Liquid cell and running the experiment, all silicon slides are thoroughly clean with a process known as "RCA Standard Clean" used in most biological experiments.[3]

The first systematically developed cleaning process for bare or oxidized silicon wafers is based on a two-step treatment with hydrogen peroxide solution: (i) an alkaline mixture at high pH followed by (ii) an acidic mixture at low pH. A preliminary clean-up treatment with a hot H_2SO_4-H_2O_2 mixture (2:1 vol) can be used for grossly contaminated wafers with visible residues. In the first treatment step, the usual volume ratios for the solution used are $5H_2O$:$1H_2O_2$:$1NH_4OH$; the mixture is known as "RCA standard clean 1 or SC-1". The usual volume ratios of the second solution are $6H_2O$:$1H_2O_2$:1HCl, which is called "RCA standard clean 2", or "SC-2". Treatments by the original immersion technique are typically 10 min at 75-80 ˚C in each solution.[12]

Large Unilamellar Vesicles (LUVs) composed of DMPC or POPC (Table 2-1, 2-2) were prepared using the extrusion technique (Figure 2-1). The phospholipids were dissolved in a chloroform and methanol mixture (9:1 vol) and transferred to a glass vial. The chloroform and methanol mixture was removed under a steam of nitrogen overnight. TBS buffer was then added directly to the dried lipid film and mixed by vortex for 10-20min to ensure a good dispersion. The lipids were reconstituted and allowed to hydrate in TBS for 4h with a spin rotator motor. The resulting large multilamellar liposomes were put through five freeze/thaw cycles using a mixture of dry ice and acetone for the freezing (Figure 2-2). Finally, the unilamellar vesicles were extruded through a 0.1μm pore size polycarbonate membrane (Nucleopore, Pleasanton, CA).

Formation of phospholipid bilayers can be described by the mechanism of vesicle fusion on hydrophilic surfaces. Vesicles initially diffuse from the bulk to the surface, where adsorption begins and proceeds until a critical concentration of absorbed vesicle is reached. Vesicles rupture and begin to spread on the surface, whereas absorbed bilayer fragments propagate the formation

of pores on unruptured vesicles. The process is completed by the lateral diffusion of bilayer fragments to minimize the hydrophobic edge energy.[13]

Imaging Ellipsometry

The ellipsometric angles and spatially resolved ellipsometric map were acquired using a commercial EP^3-SW system (Nanofilm Technologie, Göttingen, Germany). The ellipsometer (Fig.1) uses a frequency-doubled Nd:YAG laser (adjustable power up to 20 mW) at 532 nm and can be monitored by the motorized goniometer to accurately select the incident angle and the corresponding detector positions.

The ellipsometer uses a polarizer-compensator-sample analyzer nulling configuration (Figure 2-10). The polarizer and the quarter-wave plate which are located in the laser arm form an elliptically polarized incident beam. After reflection on the sample, the beam is collected through a 2× or 10× objective, via an analyzer, and is imaged by a charge-coupled device (CCD) camera. The positions of the polarizer, compensator and analyzer yield to the null condition and are then converted to the ellipsometric angles: Δ and Ψ.

For the solid-liquid cell, all measurements are taken at an incidence angle of 60˚. Silicon wafers were cut into slides to be used as substrates. The native oxide overlayer SiO_2 was measured prior to each experiment and its thickness was at an average of 15 Å. The home-built cell was used for aqueous measurements and was described in the previous paragraph.

Delta maps can be created using the mapping feature of the EP^3 View software. For this experimental configuration, Ψ is considered as constant with respect to change in Δ (Figure 2-11). Contrast images are scanned incrementally over a change in polarization angle with a constant analyzer angle. The scans are then assembled to determine the null for each point comprised of a 1.5x1.5 μm^2 region of pixels. Delta values estimated for the individual null conditions are mapped two-dimensionally and can be mapped three-dimensionally.[14]

Surface Plasmon Resonance

SPR Sample Preparation

SF10 glass slides (Schott glass, Elmsford, NY) with an index of refraction n=1.723 were cleaned using the previous RCA procedure, then rinsed with milli-Q water and dried under a nitrogen flow. To produce mechanically stable gold layers, the glass surface was covered with chromium (4 nm ± 10%) before the gold was deposited (28 nm ± 10%). The thickness of the evaporated material was measured by ellipsometry. After the formation of the gold film, the slides were soaked in a basic bath of 14:3:3 solution milli-Q water, ammonium hydroxide, and 30% hydrogen peroxide for 1 min at 65˚C. The clean gold slides were then immediately immersed in an ethanolic solution of 5mM of octadecyl mercaptan (ODM) for 16h at room temperature.[15] After mercaptan incubation, the slides were rinsed with ethanol, dried, and could be stored dust-free for several days without significant loss of quality.

SPR Enhanced Ellipsometry

The scheme of the experiment set up is shown in Figure 2-12. As for the Solid-Liquid cell, an inverse set up, with the liquid underneath the sample, is used for the SPR cell from Nanofilm Technologie (Göttingen, Germany). To get the best sensitivity a glass substrate with a gold layer is optimal. The gold-coated glass slide is assembled on a 70µL sample cell and a 60˚ SF10 prism is mounted on top of the glass slide using diiodomethane as index matching fluid. The cell has inlet and outlet tubes allowing the injection of different solutions into the cell via a peristaltic pump that allows variation of the flow rate. The laser beam passes through the prism and the substrate; it is then reflected by the metal layer. The light stimulates surface plasmon resonance in the metal film. This creates an evanescent field at the metal surface which extends into the liquid medium. The changes of optical parameters like the refractive index or thickness inside the evanescent field are in conjunction with the ellipsometric parameters Delta and Psi.The

intensity of the reflected light is measured as a function of time at a fixed angle, defined by the minimum of resonance measured previously, minus 1.5˚.

Lipid vesicles of either POPC or DMPC, prepared by extrusion, were added to the monolayer-coated substrate in the cell at a final concentration of 0.5 mg/mL lipid in TBS with a flow rate of 5 μL/min at room temperature. Fusion could be monitored by the increase of Psi which indicates an increase in thickness of the layer, and was considered to be complete when Psi reached a stable value. The change in Psi values which accompany the addition of vesicles to the alkanethiol monolayer indicates the formation of an additional layer on the electrode of a thickness which is appropriate for the expected length of the acyl chain region of phospholipid.[7] Calcium Oxalate Monohydrate (COM) seed crystals (Acros Organics, NJ) were dispersed in TBS with a concentration of 0.01 mg/mL and were added to the cell at a constant flow rate of 5 μL/min.

Optical Model for Thickness Determination

From the ellipsometric parameters, film thicknesses and interaction of COM with the lipid layer could be determined using standard classical electromagnetic theory in coordination with a parallel layer model. For the ellipsometry study using the solid-liquid cell, the model consisted of a silicon/silicon oxide/bilayer/buffer structure (Figure 2-14), and in the case of SPR enhanced ellipsometry measurement, the model consists of a SF10/Chromium/Gold/ODM and lipid monolayer structure (Figure 2-13). This process assumes that the entire sample is composed of semiinfinite parallel slabs and that each slab is composed of homogeneous material described by a single set of optical constants. Before the introduction of the phospholipid vesicles into the system, an independent ellipsometric analysis of the exact substrate structure needed to be performed in order to assign the correct substrate optical functions to analyze the lipid/substrate structure. After lipid deposition, the difference in optical function between the “bare” substrate

and lipid/substrate structure was used for the lipid thickness calculations from the final ellipsometric measurements. Refractive index values were chosen from previous reports when available. [16,17] Ellipsometric thickness averages were determined in several different locations around the center of the calculated thickness maps for each sample.

Table 2-1. Molecular structure of one of the phospholipids used in this study

1,2-Dimyristoyl-*sn*-Glycero-3-Phosphocholine (DMPC)
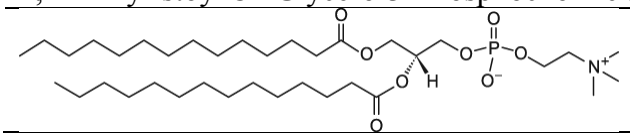

Table 2-2. Molecular structure of one of the phospholipids used in this study

1-Palmitoyl-2-Oleoyl-*sn*-Glycero-3-Phosphocholine (POPC)
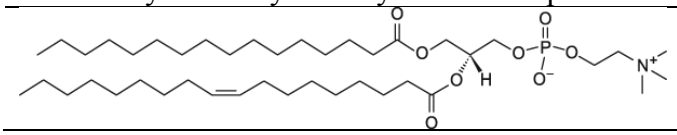

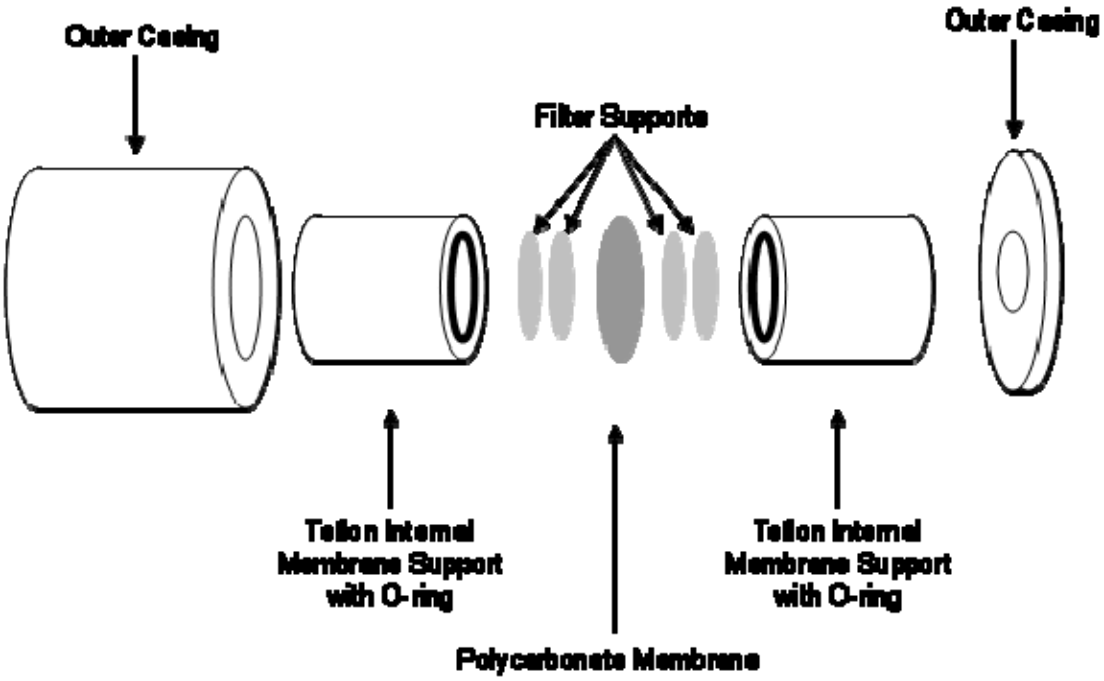

Figure 2-1. Home-made extruder used for vesicle preparation

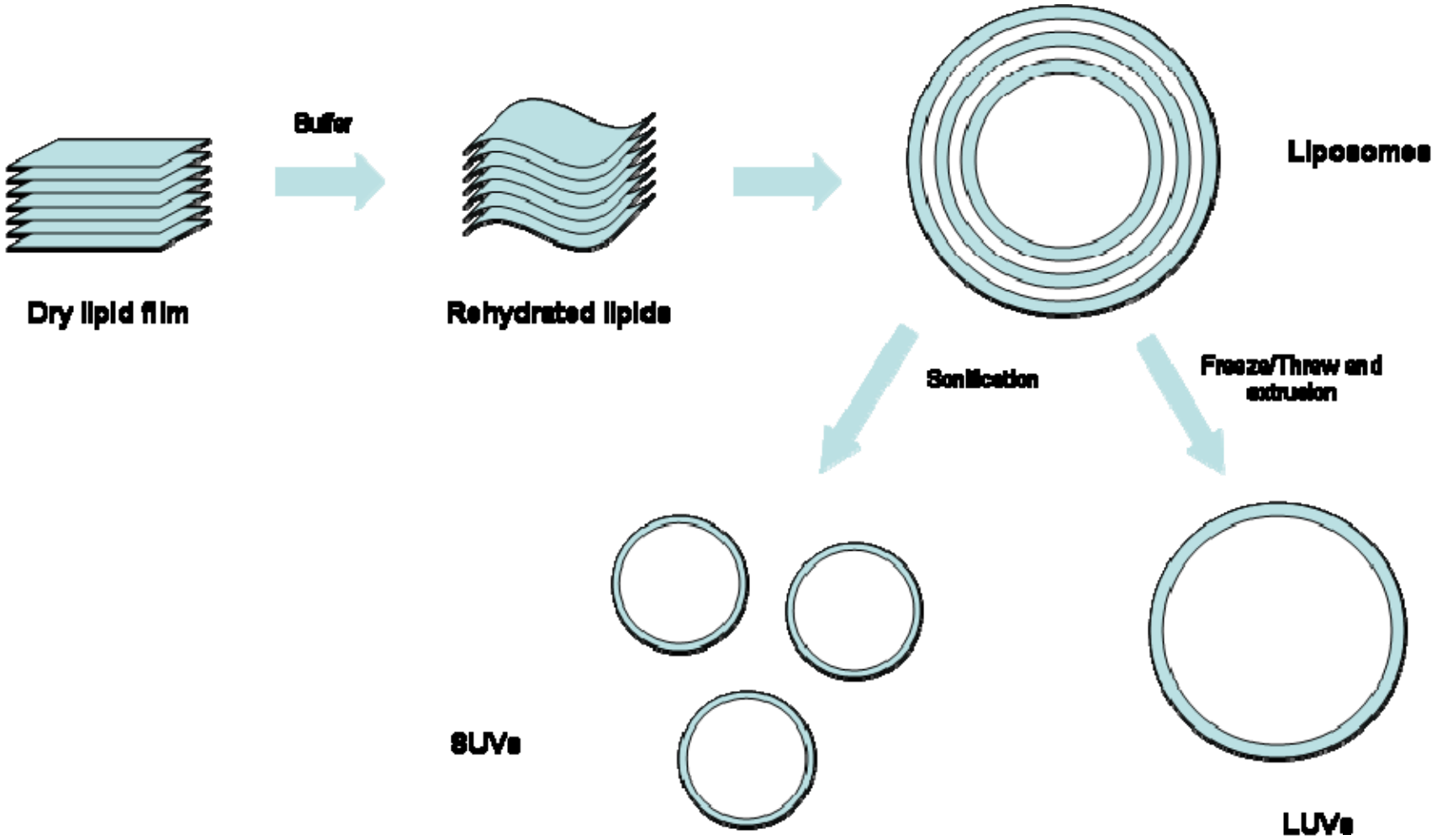

Figure 2-2. Phospholipid unilamellar vesicle preparation.

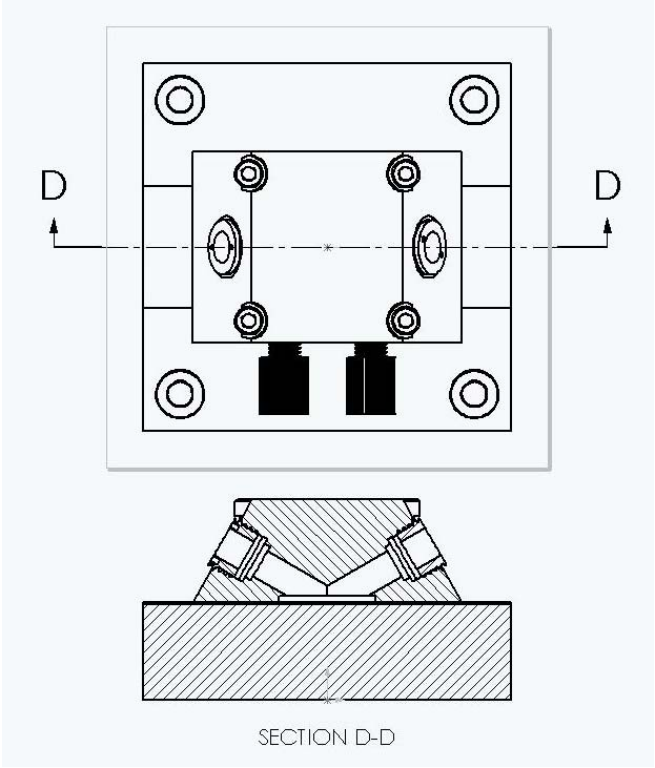

Figure 2-3. The solid-liquid cell, cut away view.

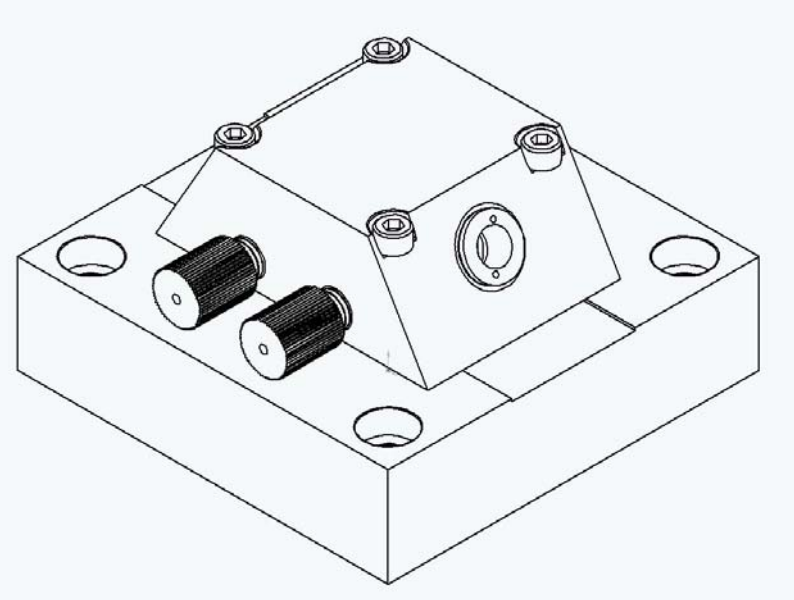

Figure 2-4. The solid-liquid cell, isometric view.

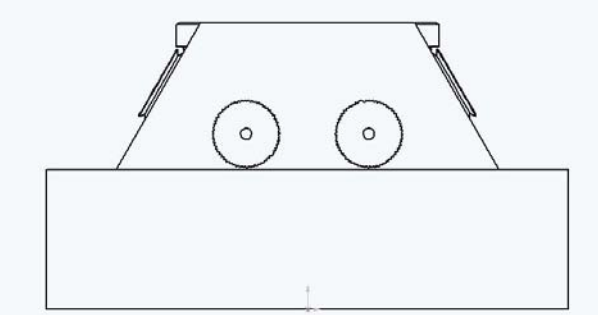

Figure 2-5. The solid-liquid cell, front view.

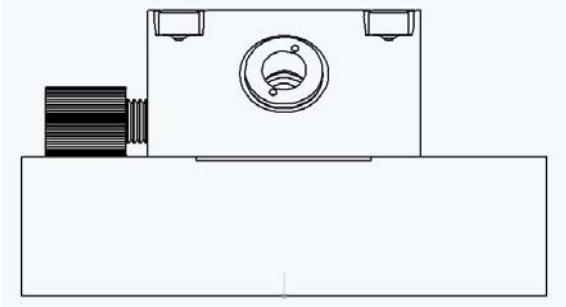

Figure 2-6. The solid-liquid cell, side view.

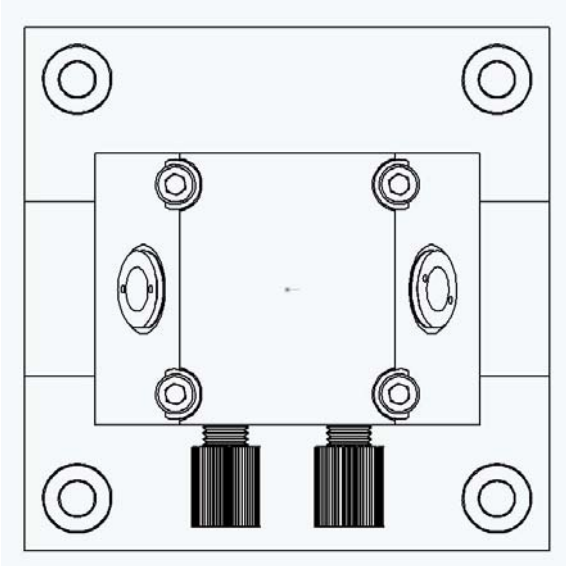

Figure 2-7. The solid-liquid cell, top view.

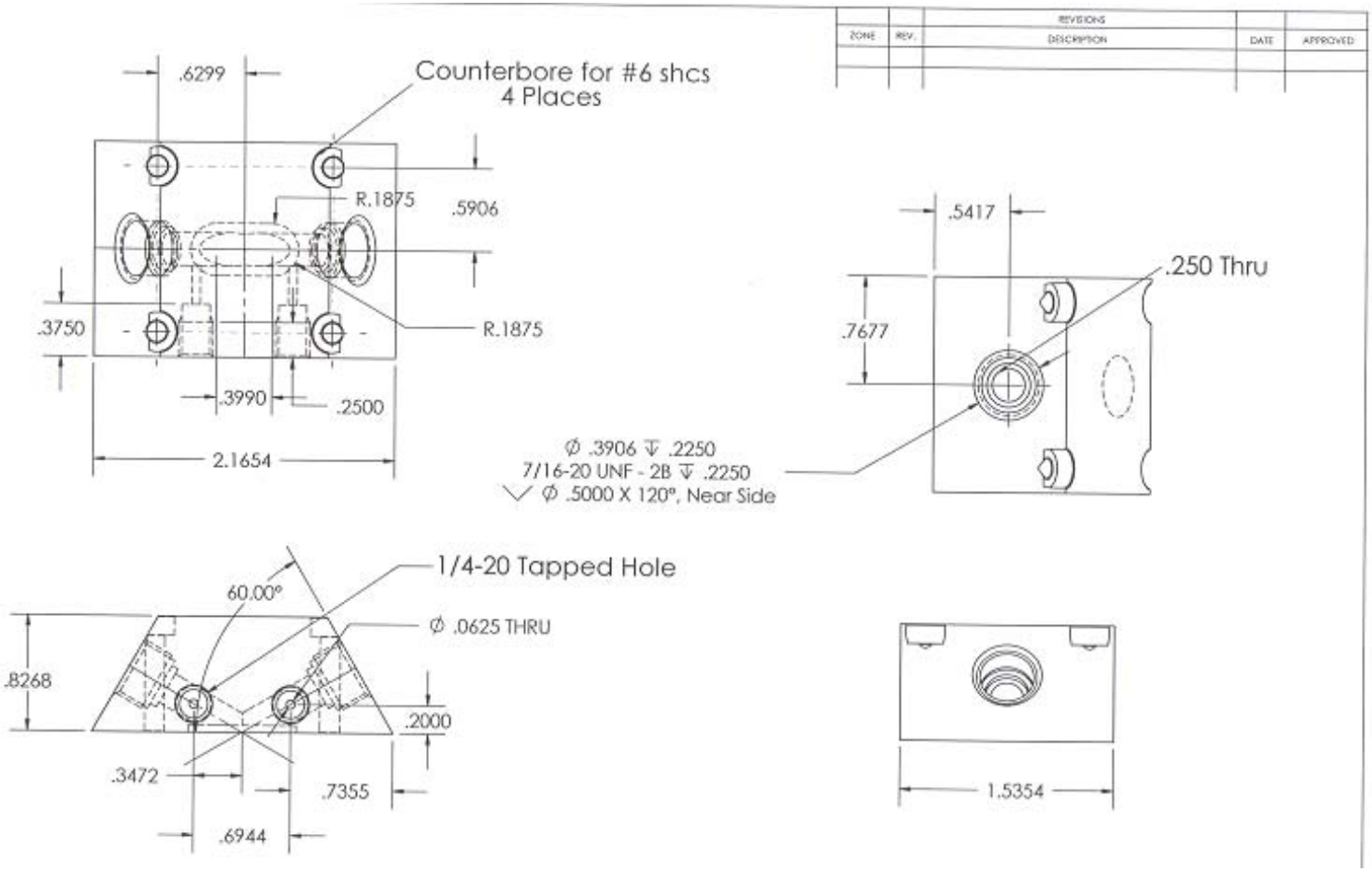

Figure 2-8. Top support drawings of solid-liquid cell in solidworks.

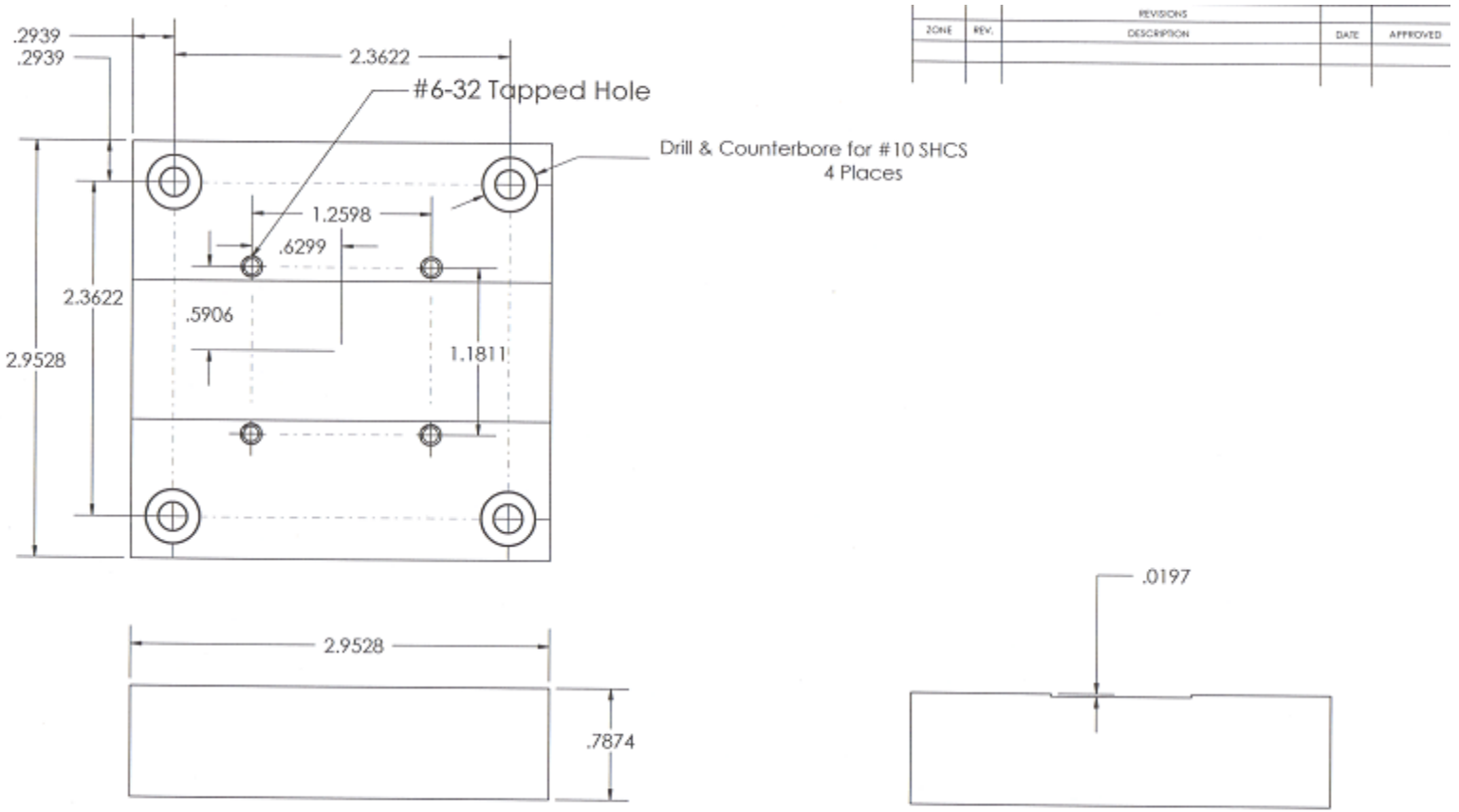

Figure 2-9. Bottom support drawings of solid-liquid in solidworks.

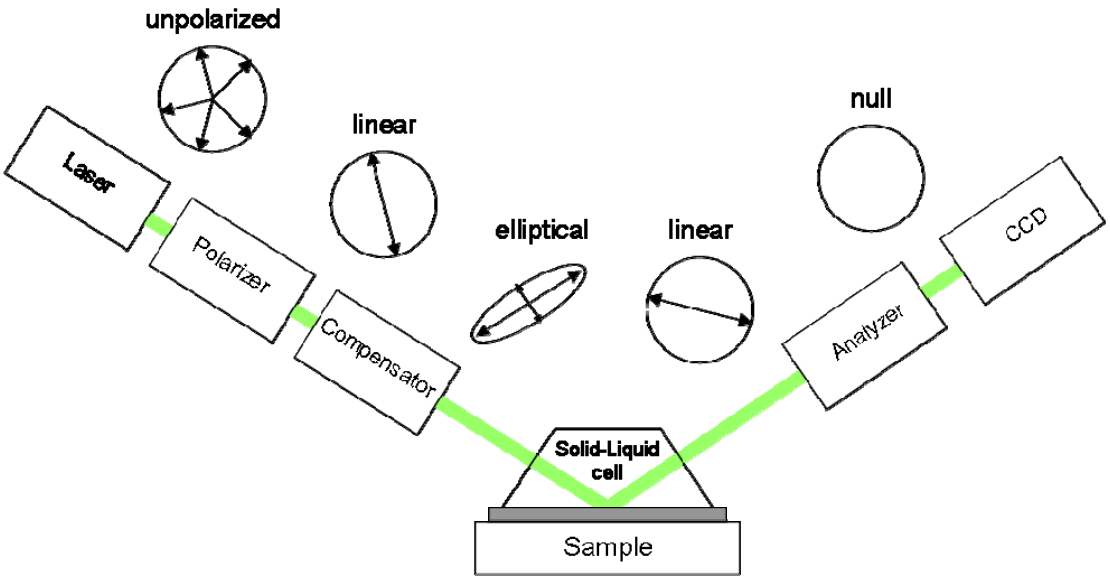

Figure 2-10. Experimental setup for ellipsometry and solid-liquid cell. Schematic description of the polarizer-compensator-sample-analyzer configuration. The BK7 windows of the solid-liquid cell are normal to the incident laser beam. Changes in polarization of the light under nulling conditions are available above.

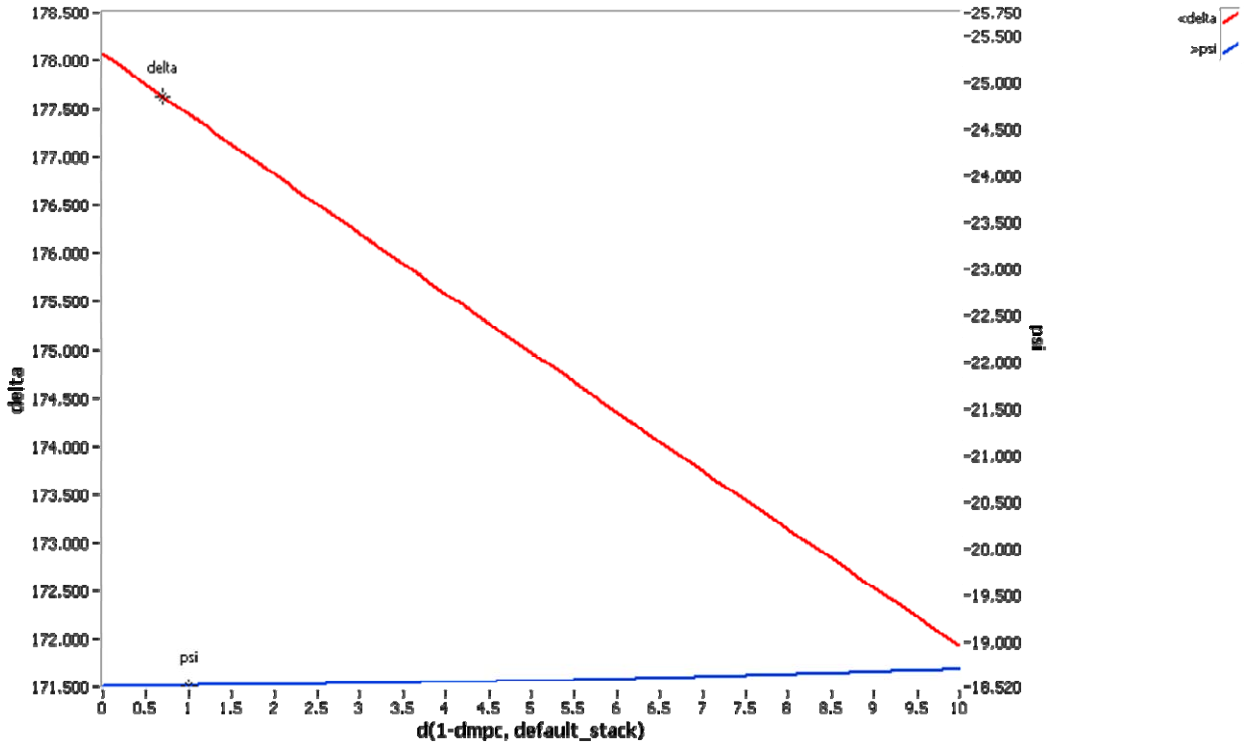

Figure 2-11. Graph of delta and psi value as function of DMPC thickness. Delta is more sensitive than psi for the use of imaging ellipsometry.

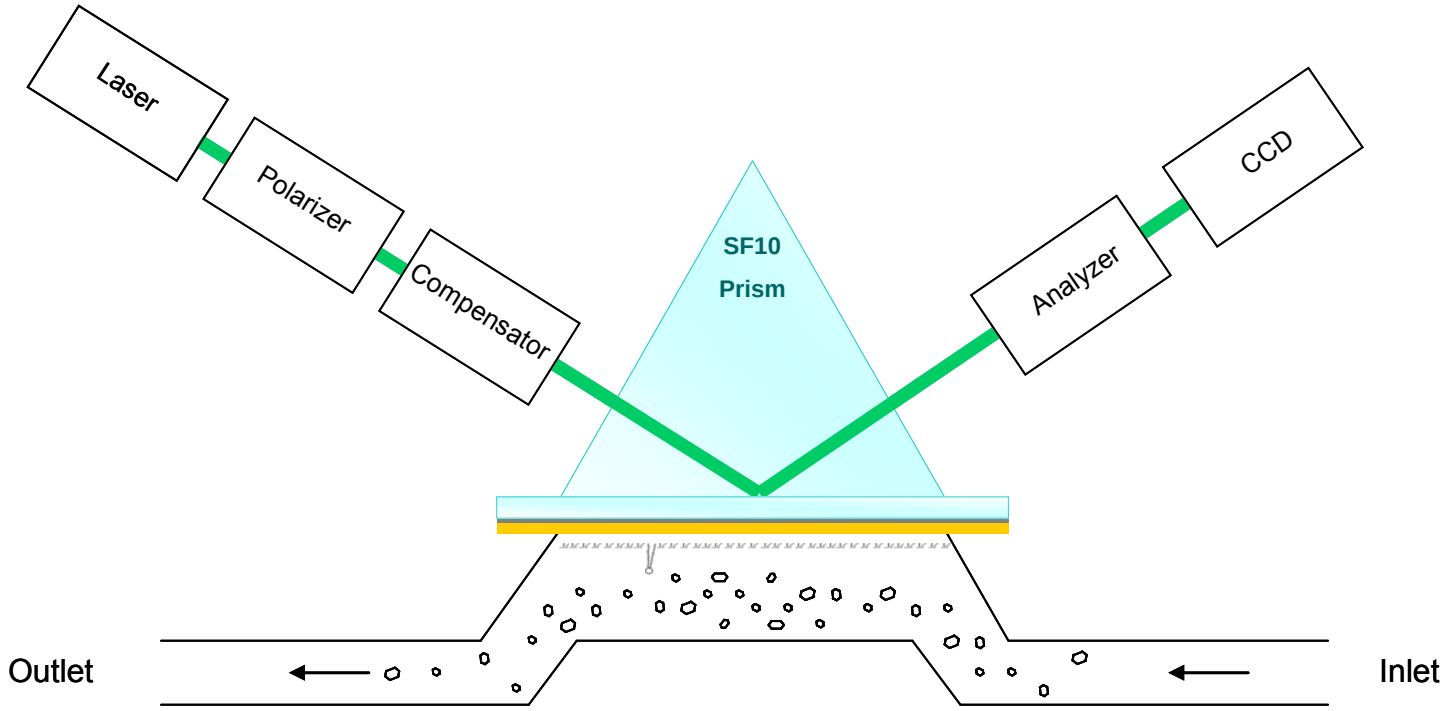

Figure 2-12. Experimental setup for SPR enhanced ellipsometry with cartoon of sample cell.

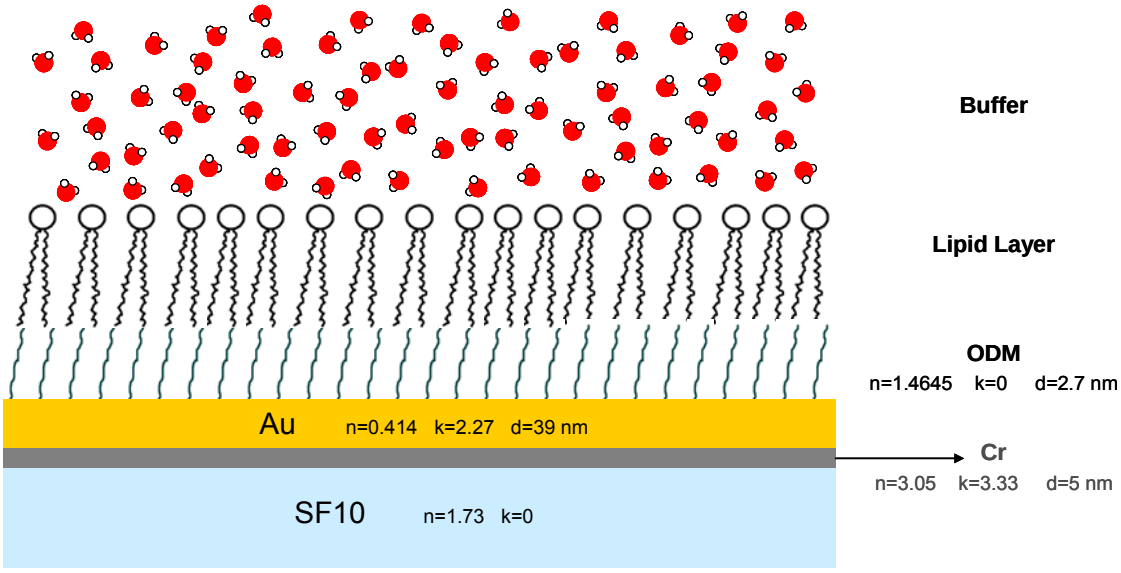

Figure 2-13. Parallel-layer model for gold slide supported phospholipid monolayer.

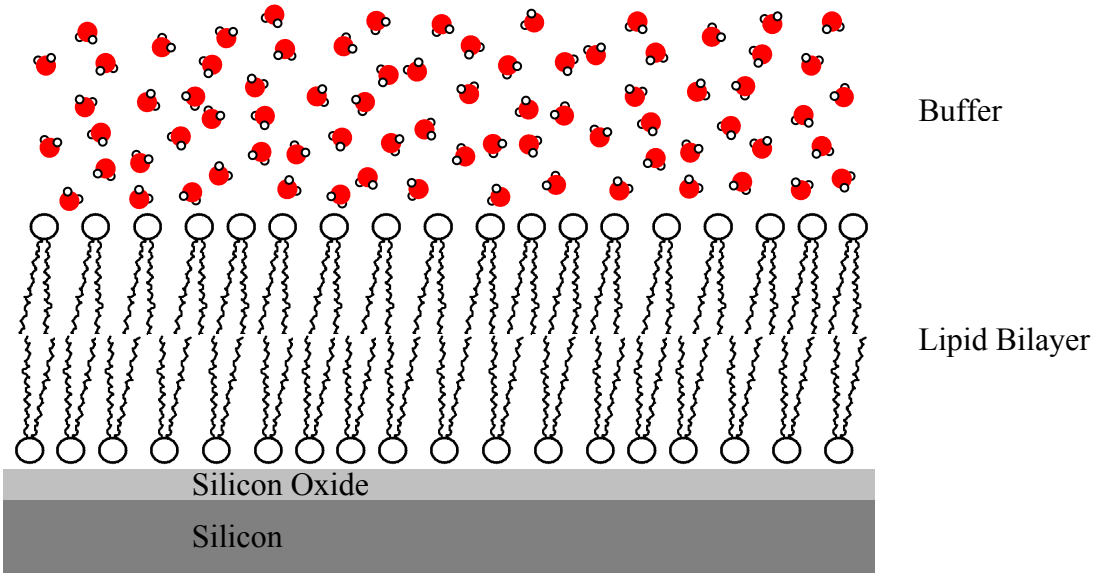

Figure 2-14. Parallel-layer model for SiO_2/Si supported phospholipid bilayer.

CHAPTER 3
RESULTS AND DISCUSSION

This chapter describes formation and quantitative measurements of bilayer thickness, uniformity and spreading of the two phospholipids used in this study, DMPC and POPC, by imaging ellipsometry and kinetic analysis in the solid-liquid cell. Further, interaction of calcium oxalate crystals in solution are measured and characterize by ellipsometry and surface plasmon resonance enhanced ellipsometry. In addition, SEM images of dried surface of silicon and gold slides used for solid-liquid interface in ellipsometry and SPR were acquired confirming the presence of COM crystals on the surface after rinsing.

Determination of Thickness of Submerged DMPC Phospholipid Bilayers by Imaging Ellipsometry in Solid-Liquid Cell

Using imaging ellipsometry, characterization of the surface coverage, lateral uniformity and film thickness of phospholipid bilayers is available. Figure 3-1 and Figure 3-2 images represent a 365 × 580 μm thickness map, derived from the spatial map of the ellipsometric angle Δ. Figure 3-1 is a thickness map of silicon dioxide on the silicon substrate and Figure 3-2 is a thickness map of DMPC bilayer added on the same surface using the refractive index (Table 3-1). Note that two scratches have been drawn (Figure 3-2) on the surface providing an optical place mark and contrast to facilitate visualization and analysis. First, the thickness map allows the measurement of the native silicon dioxide SiO_2 layer on top of the silicon (measured 1.288 ± 0.010 nm) that will be incorporated in the model to measure the thickness of the phospholipid layer. It also shows the quality and roughness of the substrate prior to the deposition of phospholipid bilayers. Second, Figure 3-1 (without scratches) and Figure 3-2 (with scratches) show the lateral uniformity and lack of defects in the DMPC bilayer over large, macroscopic areas. A slight tilt is observed on the image Figure 3-2 due to the uneven illumination. In principle, the effect can be reduced or eliminated by using a beam expander with a 2× objective,

but the solid-liquid cell is not fitted for this use. This first result is in agreement with previous work that establishes that SUVs above their transition temperatures rupture and fuse on clean silicon as well as oxidized silicon substrates to form continuous, low-defect phospholipid bilayers.[18]

In order to estimate the spatial average ellipsometric thickness for the SiO_2 native layer and DMPC bilayer we used the parallel layer model representing the sample system that consists of Buffer/SiO_2/Si and Buffer/DMPC/SiO_2/Si (see experimental section). For silicon dioxide we find 1.288 ± 0.028 nm (Figure 3-1) which is in good agreement with literature. In general, the thickness of the native amorphous silicon oxide layer on the surface of the Si wafer is about 1.0-2.0 nm.[40] for the DMPC bilayer shown in Figure 3-2 4.33 ± 0.18 nm, which is consistent with the formation of a single DMPC bilayer. In this case, we use the refractive index, n, and extinction index, k, from previous reports.[19] An independent determination of the buffer refractive index was performed using a refractometer. The ellipsometric value of 4.33 nm with a refractive index value of 1.44 for DMPC at T=30°C is in agreement with other more elaborate studies. In recent studies, *Kucerka et al.*[35-37] have estimate DMPC bilayer thickness about 4.3 nm at 30˚C using an elaborate hybrid electron-density model that analyze x-ray diffraction data for unilamellar DMPC vesicles. Also, it suggests that the choice of refractive index of 1.44 for DMPC bilayer is appropriate.

Based on this result, it is assumed that there is total surface coverage and this coverage can be calculated given that the head-group area for DMPC is known[41] to be 59 $Å^2$. Thus the maximum surface coverage is 3.84 mg/m^2 which is in agreement with values found in previous studies of DMPC.[38] In previous studies, *Stroumpoulis et al.*[38] studied the deposition and formation of DMPC by ellipsometry and estimated the surface coverage of DMPC of 3.8 mg/m^2.

Finally, these results establish that the solid-liquid cell (Figure 3-3) designed in our lab is suitable for the use of imaging ellipsometry. This technique allows for a quantitative measurement of DMPC bilayer thickness and lateral uniformity over a macroscopic area. Notably, it will be used for further application in this study including characterization of the lipid surface after the introduction of COM crystals in solution.

Kinetic Analysis for Thickness and Spreading Determination of POPC Submerged Phospholipid Bilayers

These experiments investigate the formation of a POPC phospholipid bilayer membrane by kinetic analysis. The process of vesicles fusion onto the silicon substrate is characterized as a function of time by ellipsometry in the home made solid-liquid cell that has been proved to be suitable in previous experiments. Different concentrations of POPC lipids were studied in order to choose a model of the plasma membrane as it is one of the most present phospholipid in cell membranes: 0.25 mg/mL, 0.5mg/mL, and 0.75 mg/mL.

A parallel slab layer model consisting of Buffer/POPC bilayer/SiO_2/Silicon substrate was used to fit the experimental data and calculate the thickness of the lipid bilayer. The set up and the mechanism of vesicle fusion on silicon are described in the experimental section. The analysis of binding kinetics uses a 1:1 interaction as described by the Langmuir adsorption Isotherm for first order surface adsorption. Three domains are determined and fitted by the equations:

Baseline: $f(t) = t \times 0 + constA$

Adsorption: $f(t) = f_1 \times (1 - e^{-\frac{t}{\tau}}) + constA$

Desorption: $f(t) = f_2 \times e^{-koff \times t} + constB$

Also, $kon = \frac{(\frac{1}{\tau} - koff)}{Conc.}$ and $K_D = \frac{koff}{kon}$

with t the time in seconds, τ in seconds, $Conc.$ the concentration of the lipid in solution in mol.L^{-1}, kon the association rate in s^{-1}M^{-1}, $koff$ the dissociation rate in s^{-1}, and K_D the equilibrium constant in mol.L^{-1}.

The fitting of the numerical solution of the kinetics equations to the experimental data is represented in Figure 3-4 . Measurements of Ψ as function of time is performed on randomly placed regions of interest (ROI) on the surface (ROI = 100 × 100 μm area). Figure 3-4 represents more than ten of these ROIs and shows coherence in the signal that allows us to conclude on the lateral uniformity of the formation of POPC bilayer as well as its thickness. Using our model representing the sample system, we estimate that the spatial average ellipsometric thickness for POPC bilayer is 4.6± 0.2 nm which corresponds to the value expected in the literature [19]and seems to be in accordance with the previous results of DMPC thickness. POPC has a longer lipid tail, the palmitoyl chain is a saturated –$(CH_2)_{14}$-CH_3 alkyl chain that has two more carbons than DMPC. The values found is close to the expected value, noting that the values expected for the supported lipid bilayers takes into account an orientation perpendicular to the surface.

With this new information, we assume a complete surface coverage of the POPC bilayer in all experiments and can calculate surface coverage. The average cross-sectional area of the lipid tail composed of one oleoyl and one palmitoyl chain per POPC head-group is 60.5 Å^2.[26] The surface coverage for POPC is calculated to be 4.2 mg/m^2 considering total surface coverage, which is greater than DMPC because of the greater molar mass.

Furthermore, it can be seen that the rate of the process increases with the lipid concentration, Figures 3-5 to 3-7 present in the bulk solution and that a good fit is achieved in all

cases. Table 3-2 summarizes the values of the fitting parameters τ, kon, $koff$ and K_D. The adsorption rate constant, k_{on}, is expected to be constant and independent of concentration. In fact it varies only negligibly, indicating that the simple model chosen can be used to describe this process. It is interesting to note that the equilibrium constant which represents also the effective diffusion coefficient increases with the concentration.

Moreover, $koff$ appears to increase also with concentration, mass desorption is more important at higher concentrations of POPC. In fact, initially intact vesicles adsorb until a critical concentration is reached for rupture to begin. At high concentrations, the rate at which vesicles rupture can be significantly lower than the rate at which they absorb.[38] In that procedure, more vesicles will absorb on the surface than required to form one complete bilayer and thus the excess vesicles will have to be desorbed (Figure 3-8). A vesicle is easier to desorb than a bilayer fragment because of the ratio of contact area to mass favors vesicle desorption. Finally it is important to note that $koff$ is very small at concentrations below 0.5 mg/mL because mass desorption is scarcely observable below this concentration although it is always observable at higher concentrations. We chose a simple kinetic model to fit our experimental data but it does not reflet in detail the mechanism at the surface. The model does not take into account the the diffusion limitations and different steps of vesicles adsorption. More elaborate models test some of the mechanismistic ideas for vesicle fusion by computer simulation. *Z. M. Stroumpoulis et al.*[38] have studied lipid bilayer formation with a Monte Carlo algorithm that takes into account spontaneous, adsorption and decomposition of adsorbed vesicles.

Ellipsometry Characterization of COM Crystals Interaction on Single Supported Bilayer

After characterizing the deposition of phospholipid bilayer by ellipsometry using the solid-liquid cell, we wanted to study the interaction between a solution containing calcium oxalate

monohydrate crystals and the newly formed bilayer. The suspension of COM is prepared from commercially available crystals and TBS buffer used in all experiments. COM crystals have a very low K_{sp} value of 2.3×10^{-9}, thus are easily dispersed and 0.6 mg/mL of COM crystals in suspension is used in all experiments.

Figure 3-9 shows the deposition of POPC single supported bilayers onto the silicon slide prior to the introduction of COM crystals with POPC. After injection of POPC vesicles, a change in Ψ signal is measured as a function of time. Once the system reaches equilibrium, we verify that the change in signal corresponds to the thickness of a single POPC bilayer by using the model as presented previously. The excess of vesicle remaining in the solid-liquid cell is rinsed off with TBS buffer until the signal stabilizes and no more vesicles are left. The sample cell is then filled with a suspension of COM crystals while making sure that the flow is kept constant during the experiment in order to avoid any perturbation of the phospholipid membrane. After a short period of time, a drop in the signal is observable which stabilizes quickly while solution continues to flow at constant flow rate. Even after rinsing the sample cell thoroughly with TBS buffer, it appears that crystals in solution strongly affect the quality of the responses recorded after injection of COM crystals in solution. Scattering of the light by the suspended crystals represents a limiting factor for collecting a kinetic curve of the interaction between COM crystals and POPC membrane. Nevertheless, a strong advantage of the solid-liquid cell is its ability of mapping the surface studied at a macroscopic scale.

Figure 3-10 represents a three-dimensional map of the POPC bilayer after flowing and rinsing the COM crystals in solution. Presence of multiple red spots shows a local modification in Δ signal after phospholipid being subjected to COM suspension and rinsing. Compared to previous maps of bilayer membrane, this surface is not smooth and the red spots are first

assumed to be the consequence of the adhesion of several COM crystals and aggregates on the phospholipid surface. Again we find ourselves confronted to a slight tilt on the right hand side of the image that is the result from an uneven illumination of the sample. The extended laser profile reduces the sensitivity toward one side of the image. A general problem of imaging ellipsometry is the inclined observation angle. Only a limited area of the image appears to be well-focused when using conventional optics. In principle, this limitation can be overcome by using a motorized focusing mechanism to collect a series of images with different observation angles.

A closer study of the surface will help us to identify the nature of these different patterns. Figure 3-11 allows us to get more information on the thickness and size of the multiple patterns present on the surface. A profile of thickness is measured in length (A) and width (B) of the same pattern. The profile graphs confirm the increase in thickness and give a good estimation of the length and width of the pattern. The studied structure is about 10 μm long and 5 μm width. These dimensions correspond to the range of COM crystals or aggregates. Since the buffer stays the same all through the experiments, only COM crystals are able to interact with POPC lipids and stay on the surface after rinsing even when applying strong flow up to 5 mL/min to remove any trace of COM in the bulk solution.

A complementary study is still necessary to determine the possibility of deposition of COM in the solid-liquid cell. As a consequence of the scattering light, a new system needs to be found in order to investigate the kinetics and mechanism of adhesion of COM on POPC membrane. SPR provides the means to quantify the equilibrium constants and kinetics constants in sensitive and label-free biochemical experiments. The other advantage of this technique is that the laser does not have to go through the bulk solution to detect the change in optical properties. In addition, the sample cell is in reverse position compared to the solid-liquid cell avoiding any

possibility for COM to sediment onto the phospholipid surface. Finally, SPR in combination with ellipsometry allows for the use of ellipsometric parameters giving a large enhancement of detection sensitivity in comparison to SPR techniques.[19]

Kinetic and Quantification Determination of COM Crystals Interaction by SPR Enhanced Ellipsometry

In this study, a gold metal slide is used as the metal-dielectric interface that transports the excited surface plasmon polaritons. Note that not all hydrophilic surfaces promote vesicle fusion. Surfaces of oxidized metals (e.g., TiO_2, Pt, and Au) allow the adsorption of intact vesicles but resist the formation of bilayers presumably because of weak surface interactions.[13] Hydrophobic supports, on the other hand, foster vesicle spreading by a different mechanism which consistently produces single phospholipid monolayer.[20] The gold slide was made hydrophobic by depositing an octadecyl mercaptan (ODM) layer for more than 16h.

The formation of the phospholipid layer starts by filling the sample cell with freshly produced POPC vesicles. The rupture and fusion of these vesicles was characterized as a function of time by SPR enhanced ellipsometry. The lipid adsorption mechanism onto hydrophobic surfaces is not as clear as in the case of hydrophilic surfaces, since a simple adsorption step is not possible due to the presence of the hydrophilic headgroups at the outer surface of the vesicles. Therefore, the outer leaflet of the vesicle must be split to allow the hydrophobic surface of the vesicle to rupture prior to adsorption, and finally the vesicle has to unroll and spread.

Once the system reaches equilibrium, the bulk solution is rinsed off by TBS buffer in order to remove all vesicles from the sample cell and create a baseline for the next step of the experiment. This next step is the introduction of the COM seed crystals solution onto the phospholipid membrane.

Figure 3-12 and Figure 3-13 shows first the deposition and formation of the POPC monolayer, followed by the interaction of COM with the POPC membrane. Each solution introduced in the sample cell is rinsed once equilibrium is reached. Using a six-slab model, kinetic and thickness measurements of POPC monolayer can be investigated and are presented in Table 3-3. These values are not to be compared to POPC bilayer formation, nevertheless they refer to the kinetics of deposition of a single phospholipid monolayer. Tau, τ, shows readily that the process and mechanism of a single phospholipid monolayer is much longer than a single bilayer.

After introduction of COM crystals, a rapid drop in the Δ signal confirms the first experimentation of COM crystals with the POPC membrane obtained by ellipsometry. These experiments reflect a strong and rapid interaction. Once again this phenomenon is uniform over the surface, since ten ROIs measuring the interface lipid-COM crystals in solution are randomly positioned over the surface of the cell.

The experiment is repeated with the use of a DMPC bilayer in the solid-liquid cell and DMPC monolayer in SPR cell where Δ and Ψ signal are recorded. Figure 3-14 and Figure 3-15 show the formation of DMPC bilayer in the solid-liquid cell subjected to COM crystals after equilibrium for multiples ROIs. Contrarily to POPC, the surface change observed on DMPC after rinsing COM suspension is not the same as POPC. The introduction of COM on DMPC has no consequence on the signal corresponding to the formation of DMPC. After rinsing the COM suspension from the cell that results in a little drop in signal, the signal goes back to the value corresponding to DMPC bilayer. Again scattering problems are observed and the experiment is transferred into the SPR cell. Figure 3-16 and Figure 3-17 show the formation of DMPC

monolayer onto the self-assembled ODM layer that is then subjected to COM crystals. DMPC does not undergo again a change in signal after the introduction and rinsing of COM suspension.

We consider two possible interpretation of the drop in Ψ and Δ signal for POPC membrane in both experiment SPR and ellipsometry. First, the change in signal corresponds to a partial removal of POPC membrane. Second, the change in signal corresponds to the approach and adhesion of calcium oxalate crystal onto the phospholipidic outer leaflet.

Removal of lipids can result in a drop in Ψ and Δ. For example, *H.P. Vacklin et al.* investigated the interaction of phospholipase A_2 enzyme, they showed that the enzyme played a key role in phospholipid remodeling using ellipsometry and neutron reflection.[22] The hydrolysis of phosphatidylcholine bilayers is accompanied by destruction of the bilayer at an initial rate, which was comparable for DOPC and DPPC lipids but is doubled for POPC. They proved that the enzyme penetrates into the bilayers while the amount of enzyme adsorbed at the interface is smallest for DPPC and exhibits a maximum for POPC. They observed a diminution of the bilayer thickness and surface excess as a function of time after the introduction of PLA_2. Note that PLA_2 is a heterogeneous catalyst and only acts when they absorb at a membrane surface. There is a good understanding of the enzyme-lipid interaction as well as for protein-lipid interaction. Characterization of the crystal-phospholipid interaction by ellipsometry and SPR enhanced ellipsometry has not been reported so far. Models developed for protein-lipid cannot be applied in this case. This study is the first step to the understanding of the global kinetic of the crystal-lipid interaction by ellipsometry as well as SPR enhanced ellipsometry.

A second possibility is that the signal change corresponds to adhesion of COM crystals. This results from a study by Scanning Electron Microscopy (SEM) investigating the presence of

COM crystals after experiment, calculations in signal change support and investigation of the influence of COM optical properties all support the adhesion hypothesis.

A complementary study by SEM shows the presence of calcium oxalate monohydrate crystals after rinsing the COM suspension from the cell. Figure 3-18 and Figure 3-19 show SEM images of COM crystals found after removal of both the solid-liquid and SPR cell superior support. After experimentation, silicon and gold slides are left to dry in a dust free environment at ambient temperature for at least overnight. SEM images reveal the presence of COM crystals on silicon and gold slides surrounded by NaCl crystals and Tris HCl crystals dissolved in TBS buffer prior to the drying procedure. COM crystals are recognizable by their structure and form. Figure 3-18 (A) also shows the plate-like crystals characteristic of the morphology of COM. Plate-like angles are close to 120˚ in agreement with prior studies.[6, 24] Most crystals present their (100) face (Figure 3-20) that is perpendicular to the microscope view.[5] The SEM data that clearly show presence of adsorbed crystals suggest that the first hypothesis that the change in SPR signal is due to the removal of phospholipids is less probable.

Moreover, both ellipsometry and SPR enhanced ellipsometry experiments shows a change in Δ and Ψ signal, for POPC membrane. Table 3-4 presents the ratio of the signal change caused by COM crystals over the signal change caused by either the POPC bilayer formation or POPC monolayer formation. The signal change caused by COM crystals on POPC bilayer is 32.9% and the signal change caused by COM crystals on the POPC monolayer is 63.6%. This relation of proportionality of 2 between the change of signal caused by COM crystals from a bilayer to a monolayer shows the concordance of the phenomenon on the outer leaflet of POPC. The same amount of change in phospholipid-crystal interface is observed in both monolayer and bilayer for POPC. Suggestion that the phospholipid membrane is partially removed while continuing

flowing COM suspension is not retained. Though, suggestion that adhesion of COM crystals onto the outer leaflet of a phospholipid membrane cause the same signal change is much more probable.

Further support for adhesion is that a decrease in signal observed is caused by the optical properties of COM. Note that a decrease in signal is first observed when introducing COM crystals in the bulk solution after rinsing the sample cell of remaining DMPC vesicles. A complementary study on the effect of the introduction of COM crystals in solution onto a hydrophobic self-assembled monolayer (ODM) and a bare gold surface is presented in Figure 3-21 and Figure 3-22 respectively.

Once the COM crystals are introduced in the sample cell, the Ψ signal decreases about 0.08 degrees. This blank experiment shows the effect of the change in optical properties in the bulk solution on the Ψ signal. Initially filled with TBS buffer, the sample cell that supports the bare gold slide is replaced with COM crystals in solution, and as a consequence the signal immediately decreases of 0.08 degrees of Ψ. This signal change corresponds also to the change when rinsing the sample cell containing COM crystals in bulk solution in POPC and DMPC experiments. More importantly the irreversible adsorption of COM crystals on a hydrophobic, uncharged surface (ODM) promotes the hypothesis that COM crystals are partially interacting with the hydrophobic chain region of phospholipid bilayers during adhesion.

Analysis of the results by SEM, calculation of signal change and interpretation of the effect of COM optical properties, suggest that the second hypothesis of COM adhesion onto phospholipid membrane is preferred compared to the hypothesis of a partial removal of the phospholipid membrane. Further model and interpretation are needed and will allow the confirmation of this hypothesis.

Finally, kinetic of the interaction between crystal and lipid is calculated and the influence of the nature of the phospholipid membrane is also observed. The initial rate of decrease of POPC phospholipid represented by *koff* was analyzed using a linear curve fit and found to be $4.49 \times 10^{-2}\ s^{-1}$. When membrane is composed of DMPC the signal does not undergo such a change, after rinsing the COM suspension from the SPR and SL cell, Δ and Ψ signal retrieve the signal corresponding to a bilayer or monolayer presence (Figure 3-14 through 3-17). These data are qualitatively fitted to estimate the changes in surface coverage during the adhesion and to obtain a qualitative picture of the initial interaction of COM crystals with phospholipids.

The difference in response when introducing COM crystals between DMPC and POPC membranes shows that a difference in lipid chains has a regulating effect on the interaction. The commercially available COM crystals seem to have a strong interaction with POPC contrarily to DMPC. Contrarily to POPC, DMPC does not retain or attach COM crystals used in this study. COM crystals interact very differently with POPC and DMPC due to the different structural characteristics of the phospholipids. The lipids have the same head-group but different tail chain and membrane density. In fact, POPC has a longer and one unsaturated tail group compare to DMPC. Moreover, the POPC bilayer has initially a lower mean density than DMPC that should create more room for the COM crystals to interact with the membrane thus interacts more easily with POPC. The composition of the tail group has an important influence on the headgroup and significantly modulates lipid diffusion. Lipid fluidity plays an important role in cellular processes as cells adhesion.[39] POPC and DMPC have the same headgroup PC (see Table 2-1), the PC interface is modified by the nature of the tail chain. The negatively charged oxygen and the esters become more accessible to the predominantly and positively charged face (100) of COM crystal. POPC has already been proven to induce nucleation and adhere COM crystals

contrarily to DMPC. In Figure 3-23 the interaction of a COM crystal with phospholipids is modeled with the COM crystal adhering to the outer headgroup region of the phospholipid monolayer.

In a previous work, *S.R. Kahn et al.* already proved the effect of packing density of the headgroup on crystal formation.[25] In this study, they observed that lower packing density generated more crystals. Plus crystal attachment to the inner medullary collecting duct cells has previously been correlated with membrane fluidity. Finally, membrane damage, which is so prevalent after exposure to oxalate and COM crystals, may lead to exceptionally fluid sited that can catalyze crystal adhesion. Our observations confirm this different theory. Not only is our approach to analyze COM adhesion is novel but it also provides us of new information concerning this interaction.

As there is a large contrast between different phospholipids, the interaction COM crystal-tail chain plays a crucial role in the COM crystal process adhesion. Insight into the mechanism of the attachment can be investigated and complemented using other techniques that would resolve depth profile of the movement normal to the surface. Building an optical model adapted to the diffusion of a heterogeneous suspension and the adhesion of crystals onto a uniform layer is the following step that will allow extraction of desired information and transforming directly Δ and Ψ signal into the mass of COM crystal attached on the phospholipid interface and its repartition. This new approach represents a further step in the understanding of the mechanism of COM crystal adhesion, its consequences and the parameters regulating the adhesion. Our work is another step towards understanding kidney stone formation.

Table 3-1. Refractive and extinction index of SiO_2 and DMPC with their respective thickness.

Layers	Refractive index n	Extinctive index k	Thickness (nm)
Silicon Dioxide	3.88	2.05	1.29
DMPC	1.44	0	4.33

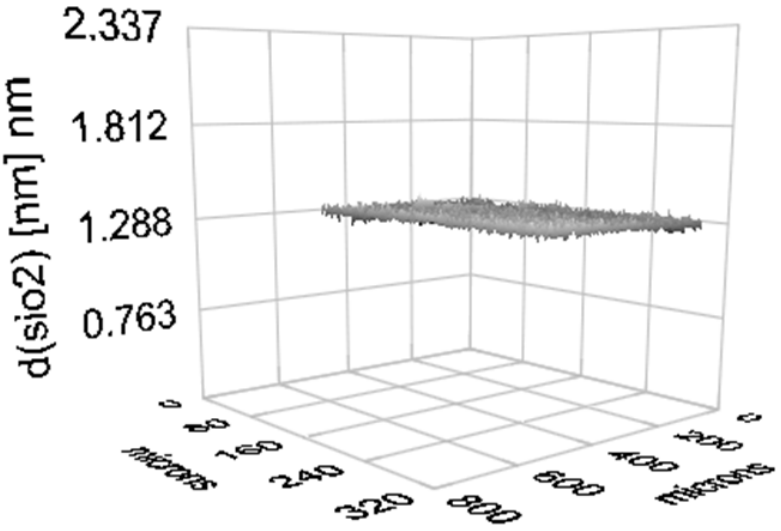

Figure 3-1. Three-dimensional thickness map of silicon dioxide surface by imaging ellipsometry.

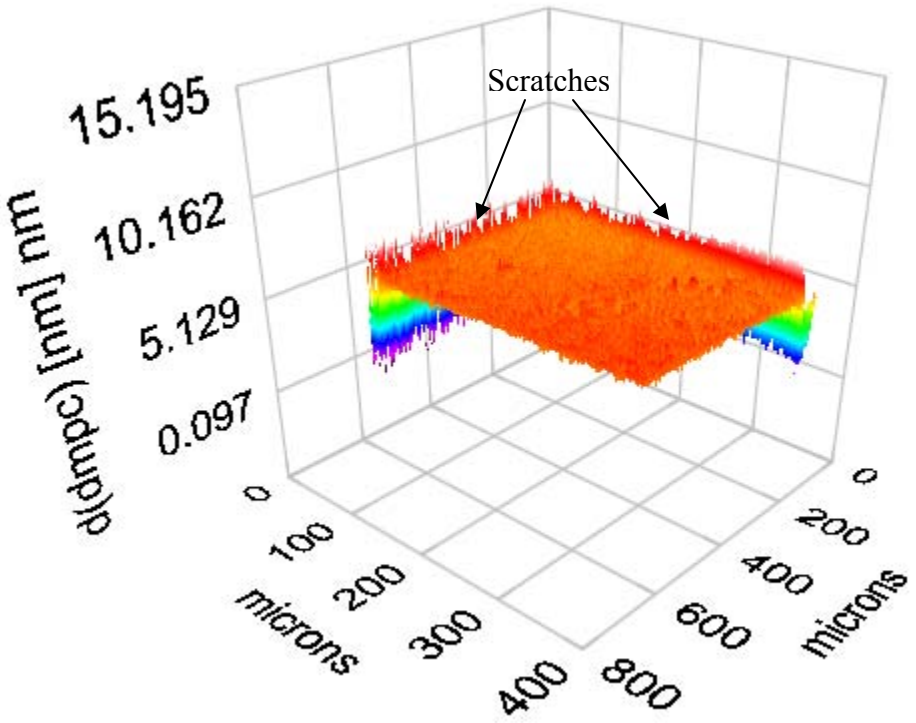

Figure 3-2. Three-dimensional thickness map of DMPC bilayer on silicon/ silicon dioxide substrate. Two scratches have been made before deposition of the lipid.

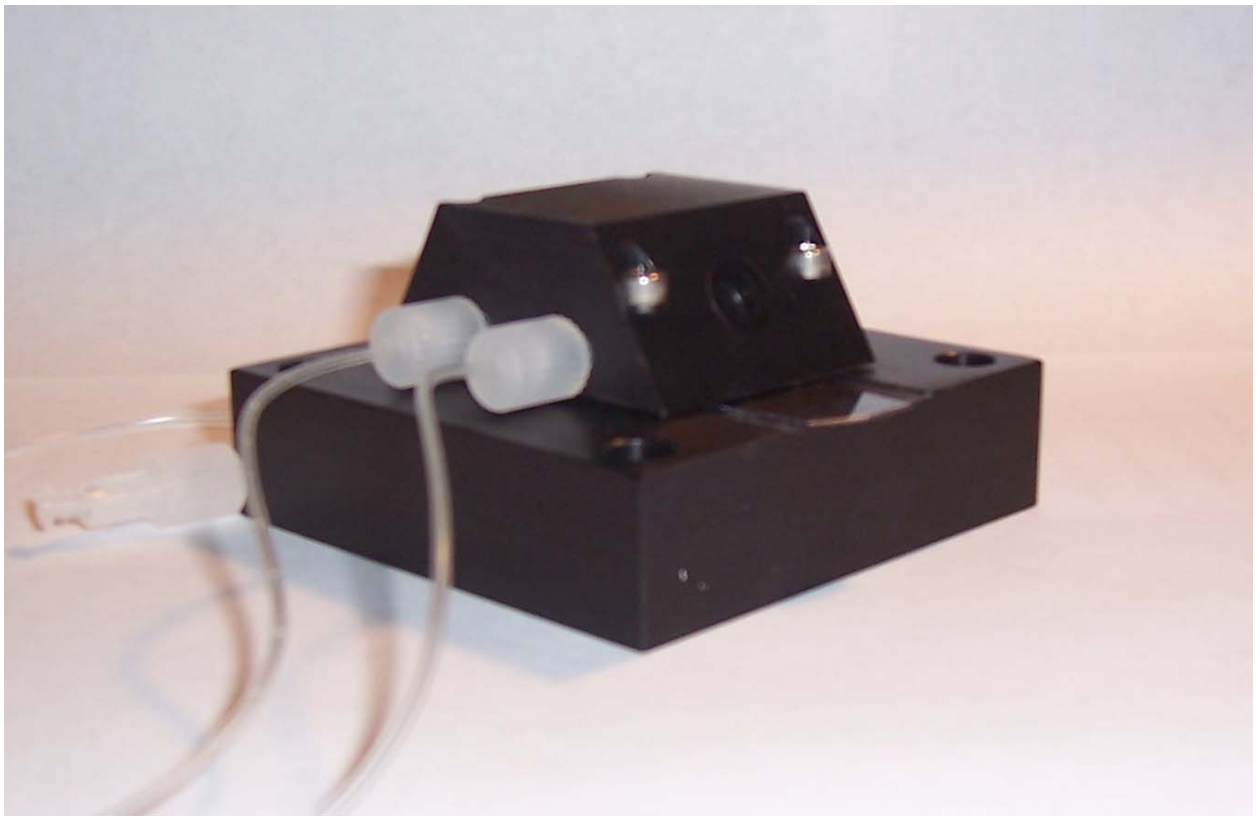

Figure 3-3. Home made solid-liquid cell.

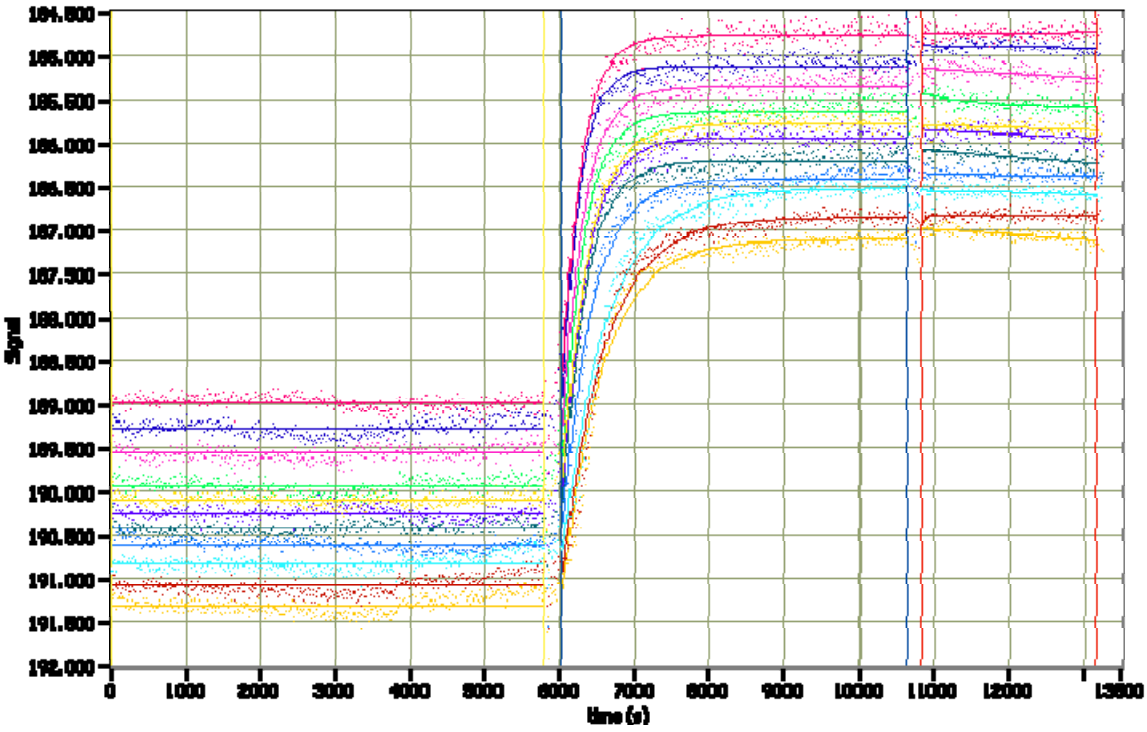

Figure 3-4. Real-time measurement of POPC bilayer formation on silicon substrate in solid-liquid cell. Δ signal recorded with ten ROIs as a function of time (angle of incidence 60˚).

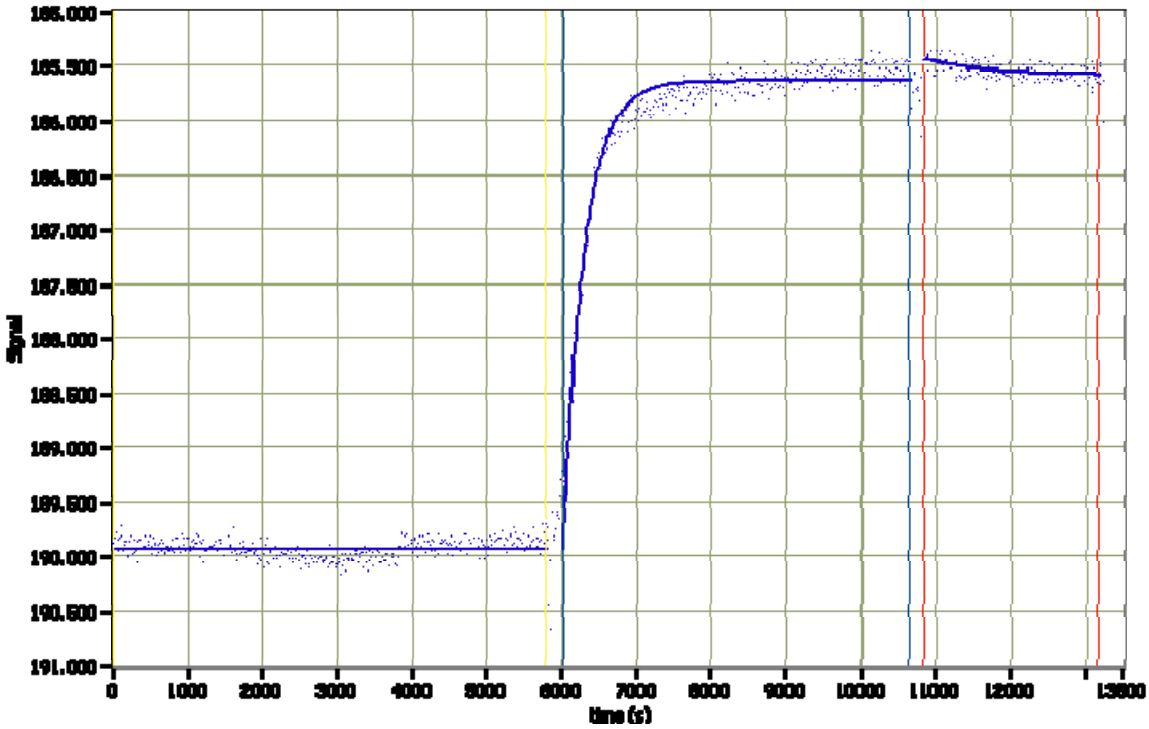

Figure 3-5. Real-time measurement of 0.75 mg/mL POPC bilayer formation on silicon substrate in solid-liquid cell. Δ signal recorded as a function of time (angle of incidence 60˚).

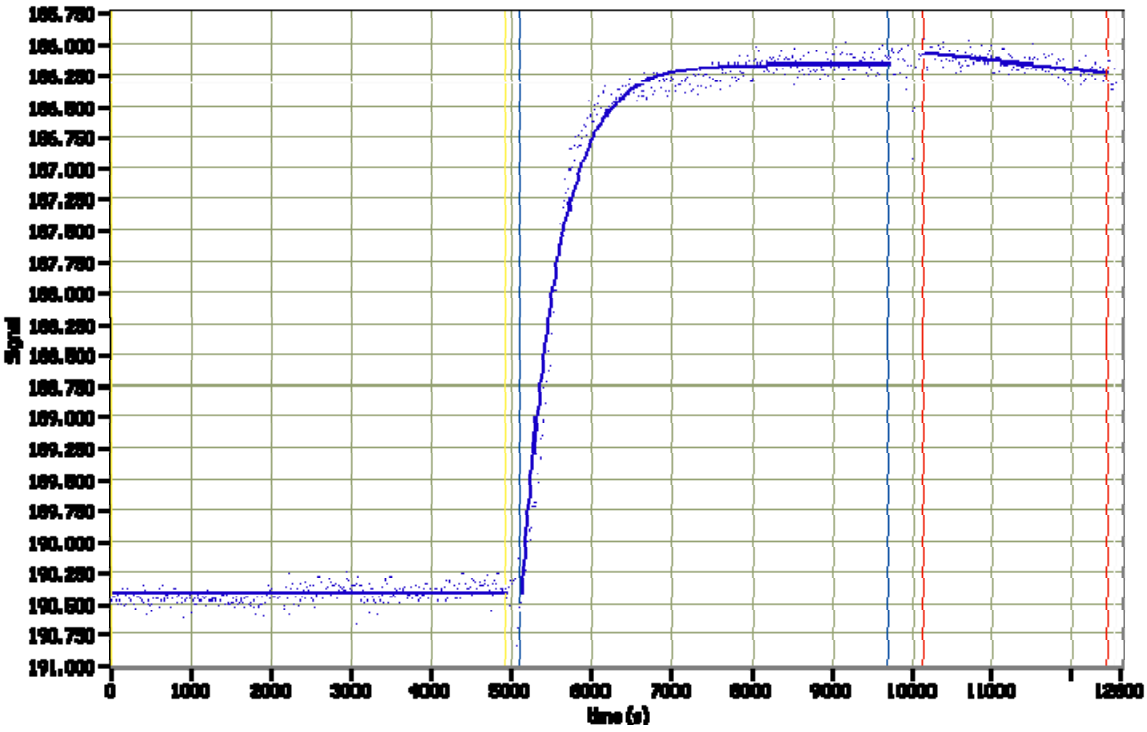

Figure 3-6. Real-time measurement of 0.5 mg/mL POPC bilayer formation on silicon substrate in solid-liquid cell. Δ signal recorded as a function of time (angle of incidence 60˚).

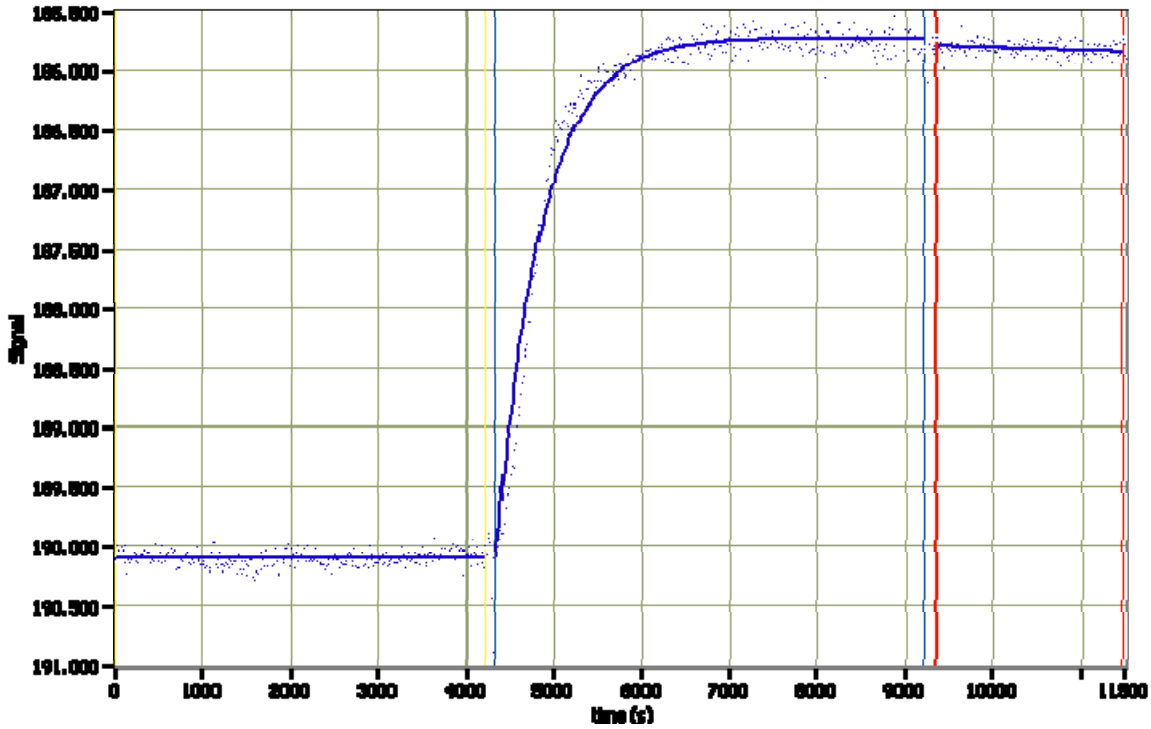

Figure 3-7. Real-time measurement of 0.25 mg/mL POPC bilayer formation on silicon substrate in solid-liquid cell. Δ signal recorded as a function of time (angle of incidence 60˚).

Table 3-2. Estimated kinetic parameters values for the fitted experimental data to model for POPC vesicle fusion onto silicon substrate in solid-liquid cell.

Lipid concentration Conc. (mg/mL)	Tangential constant τ (s)	Adsorption Rate constant *kon* ($s^{-1}M^{-1}$)	Desorption Rate constant *koff* (s^{-1})	Equilibrium constant K_D (M)
0.75	284.48	4.554×10^{-3}	1.00×10^{-4}	2.1961×10^{-2}
0.5	412.37	4.829×10^{-3}	1.26×10^{-5}	2.609×10^{-3}
0.25	768.54	4.724×10^{-3}	7.00×10^{-6}	1.463×10^{-3}

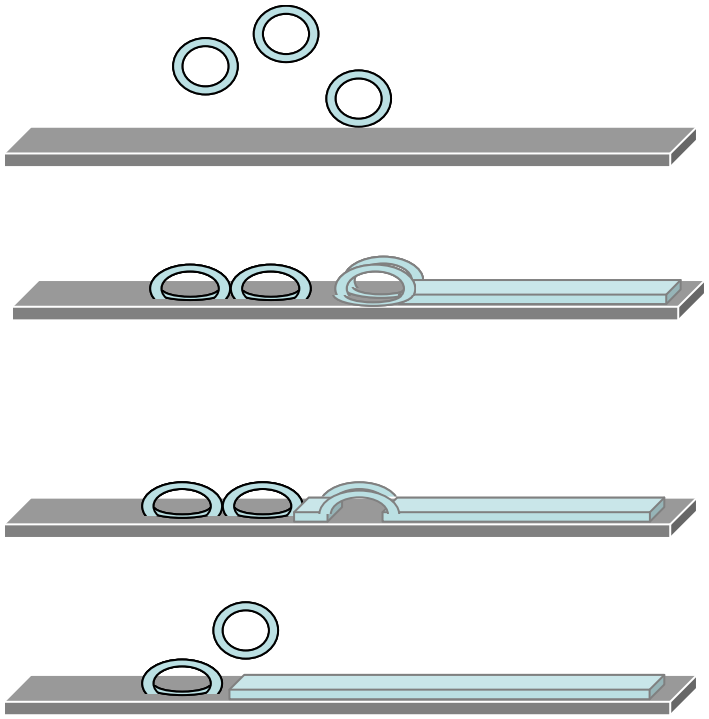

Figure 3-8. Schematic showing how a ruptured vesicle can insert itself under an intact vesicle decreasing its contact area and forcing the intact vesicle off the surface.

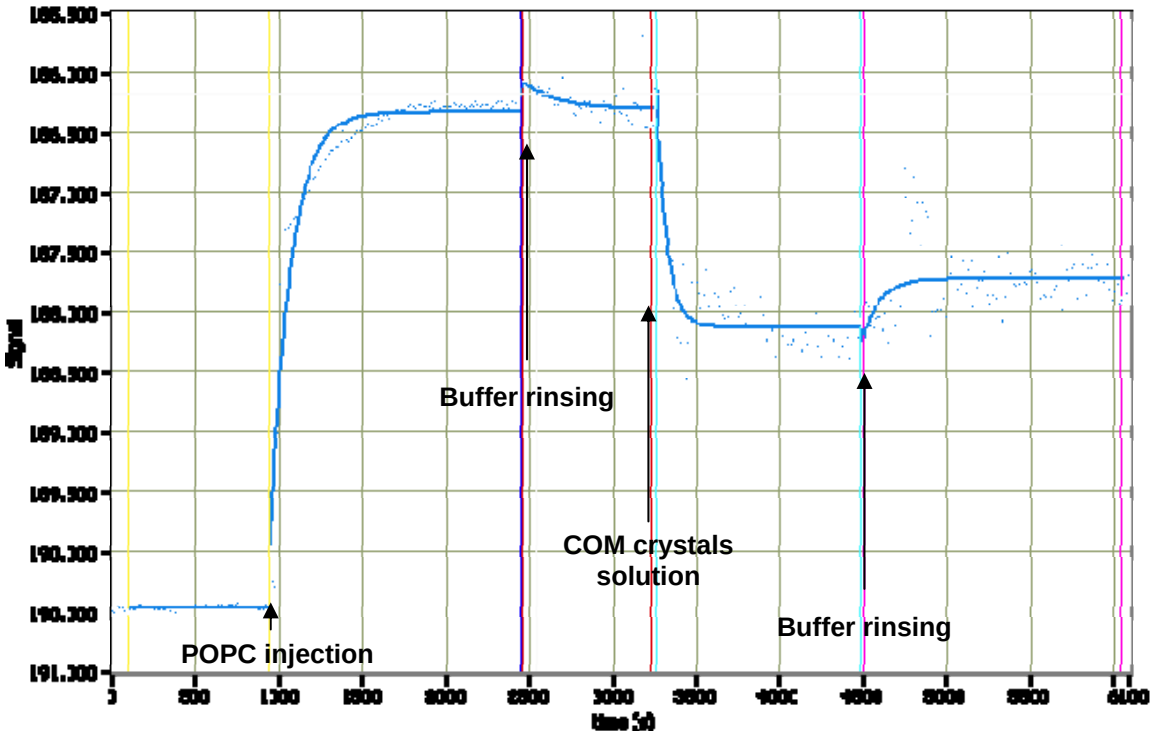

Figure 3-9. Real-time measurement of 0.75 mg/mL POPC bilayer formation followed by the introduction of COM crystals in TBS buffer in solid-liquid cell. Δ signal recorded as a function of time (angle of incidence 60˚).

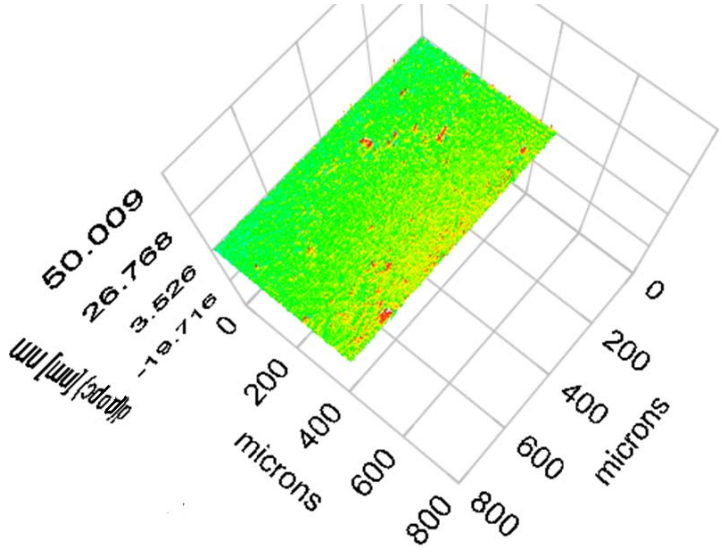

Figure 3-10. Three-dimensional thickness map of POPC bilayer spread on silicon substrate in solid-liquid cell after introduction of COM crystals and rinsing with TBS buffer.

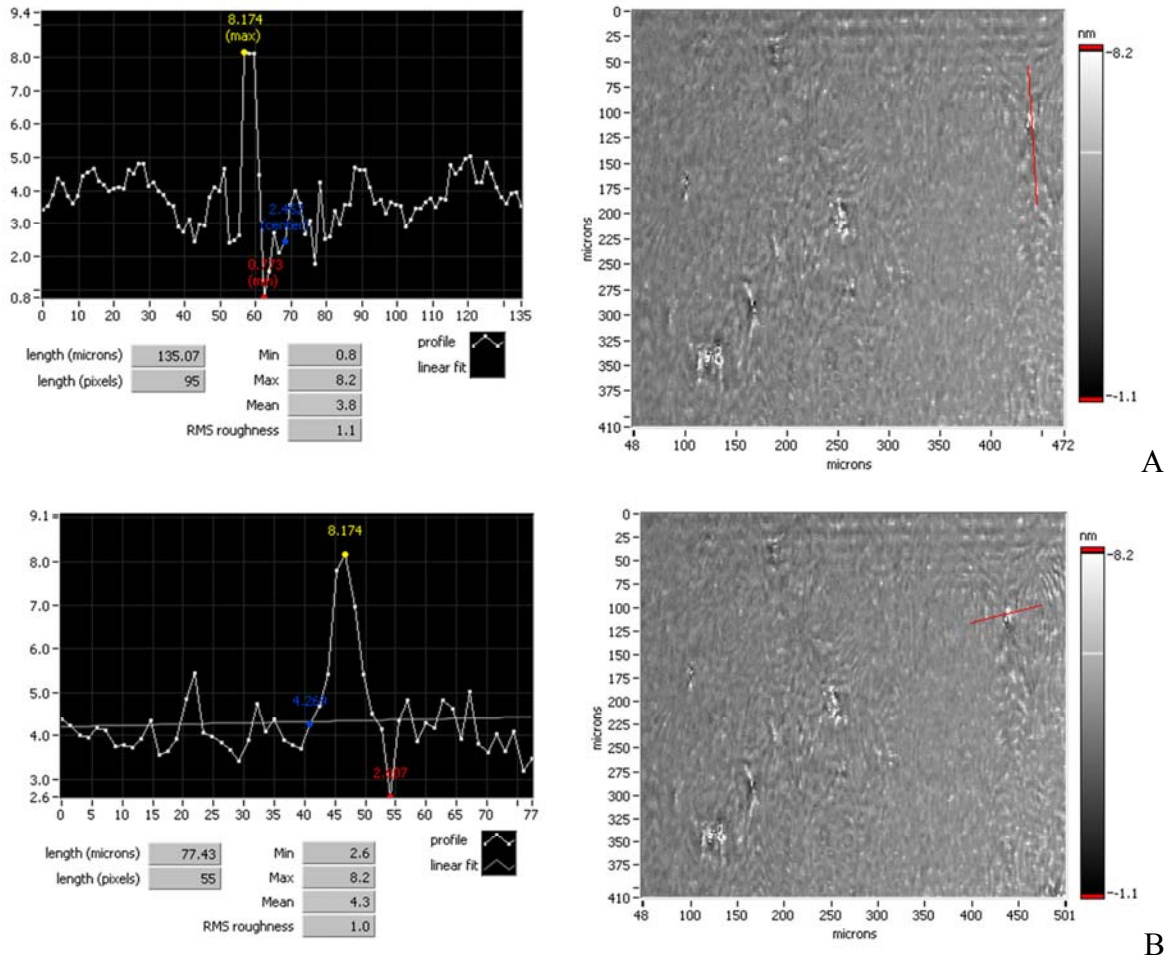

Figure 3-11. Spatially resolved map of ellipsometric angle, Δ, of POPC bilayer surface after introduction COM crystals and rinsing with TBS buffer. A) Profile of a bright spot in length, B) width.

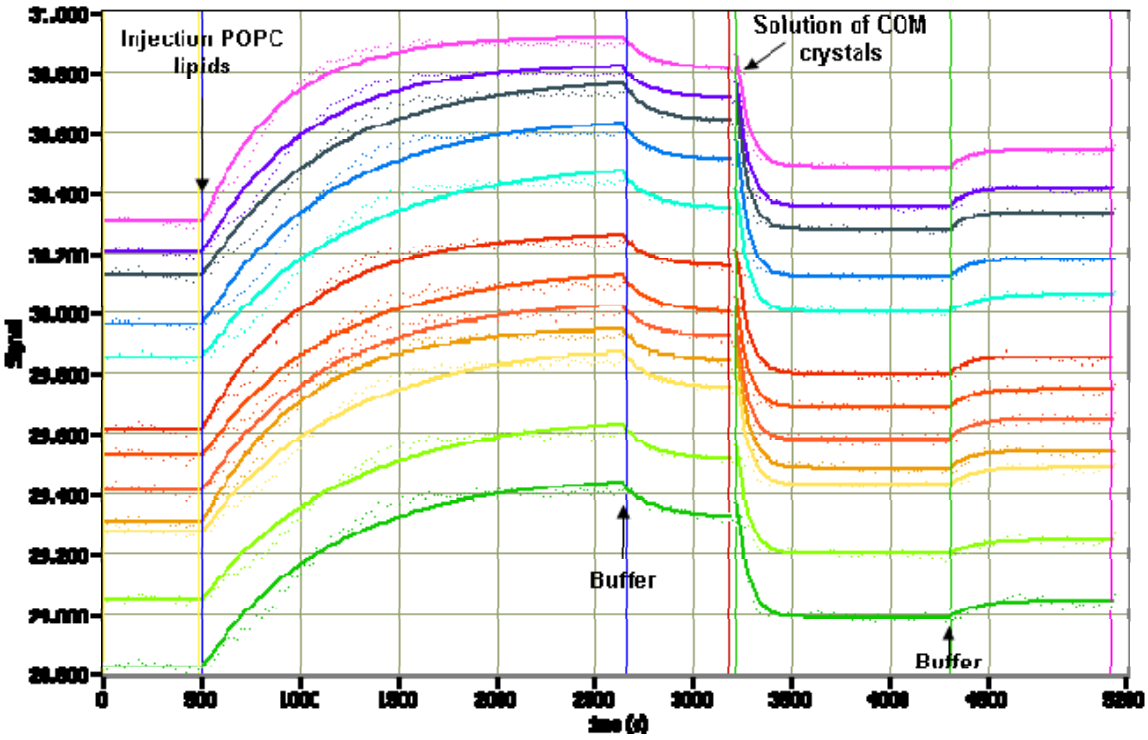

Figure 3-12. Real-time measurement of POPC monolayer formation on ODM followed by the introduction of COM crystals. Ψ signal recorded with ten ROIs as a function of time with SPR cell.

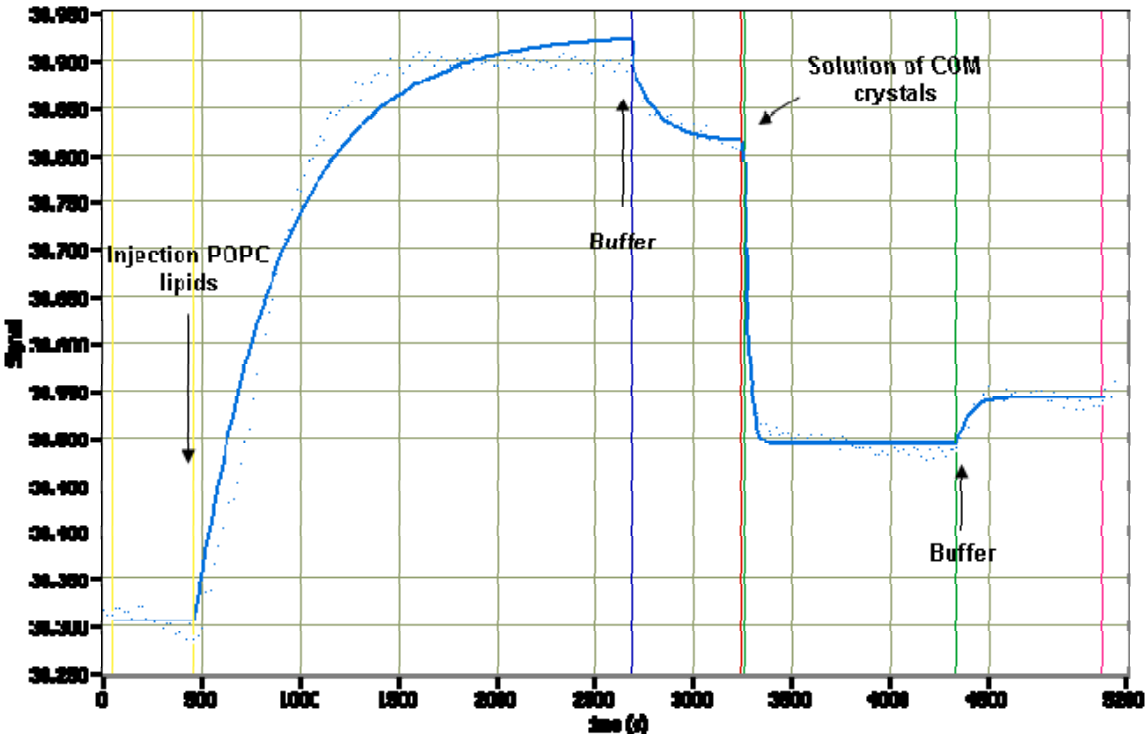

Figure 3-13. Real-time measurement of POPC monolayer formation on ODM followed by the introduction of COM crystals. Ψ signal recorded as a function of time with SPR cell.

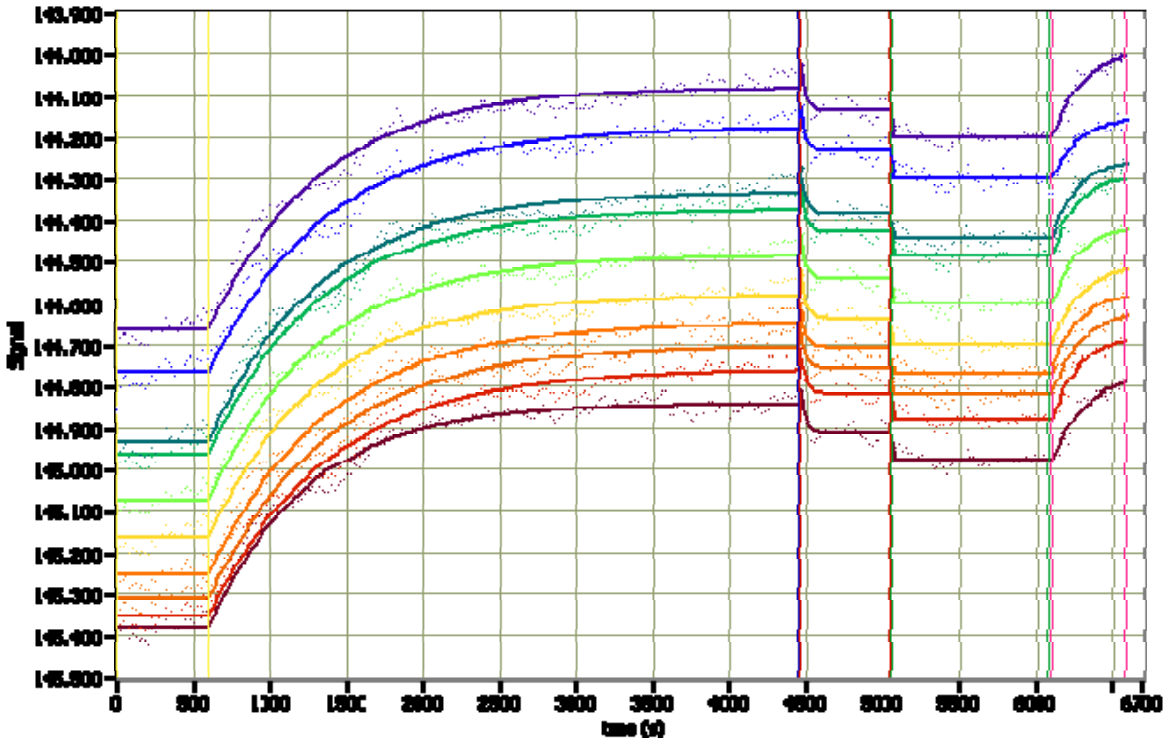

Figure 3-14. Real-time measurement of DMPC monolayer formation on ODM followed by the introduction of COM crystals. Δ signal recorded as a function of time with solid-liquid cell.

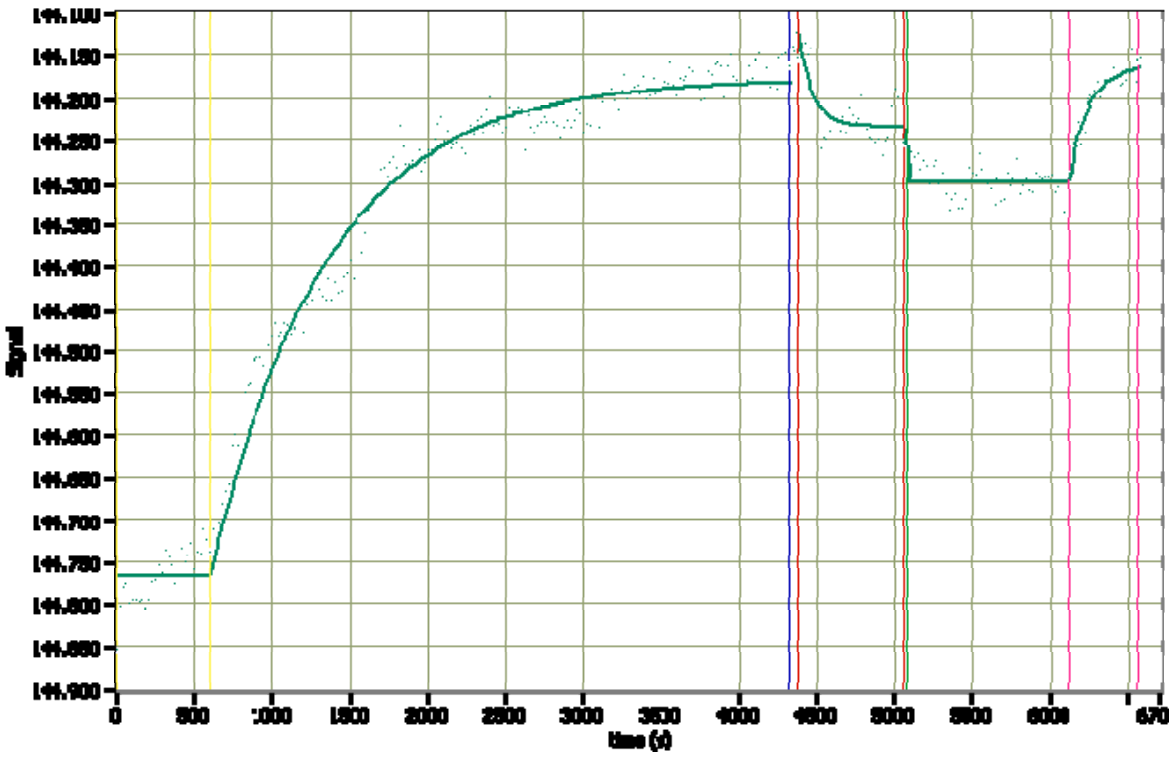

Figure 3-15. Real-time measurement of DMPC bilayer formation on silicon substrate followed by introduction of COM crystals in solid-liquid cell. Δ signal recorded as a function of time (angle of incidence 60˚).

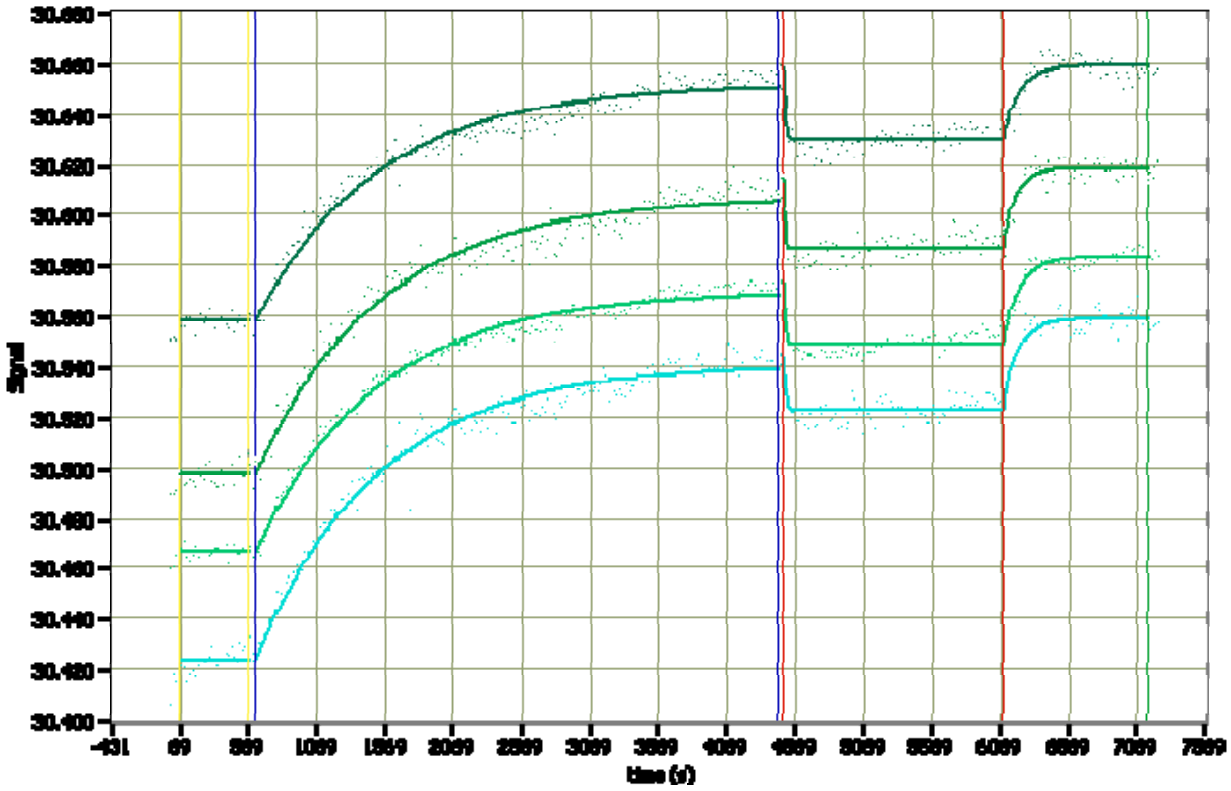

Figure 3-16. Real-time measurement of DMPC bilayer formation on silicon substrate followed by introduction of COM crystals in SPR cell. Ψ signal recorded as a function of time.

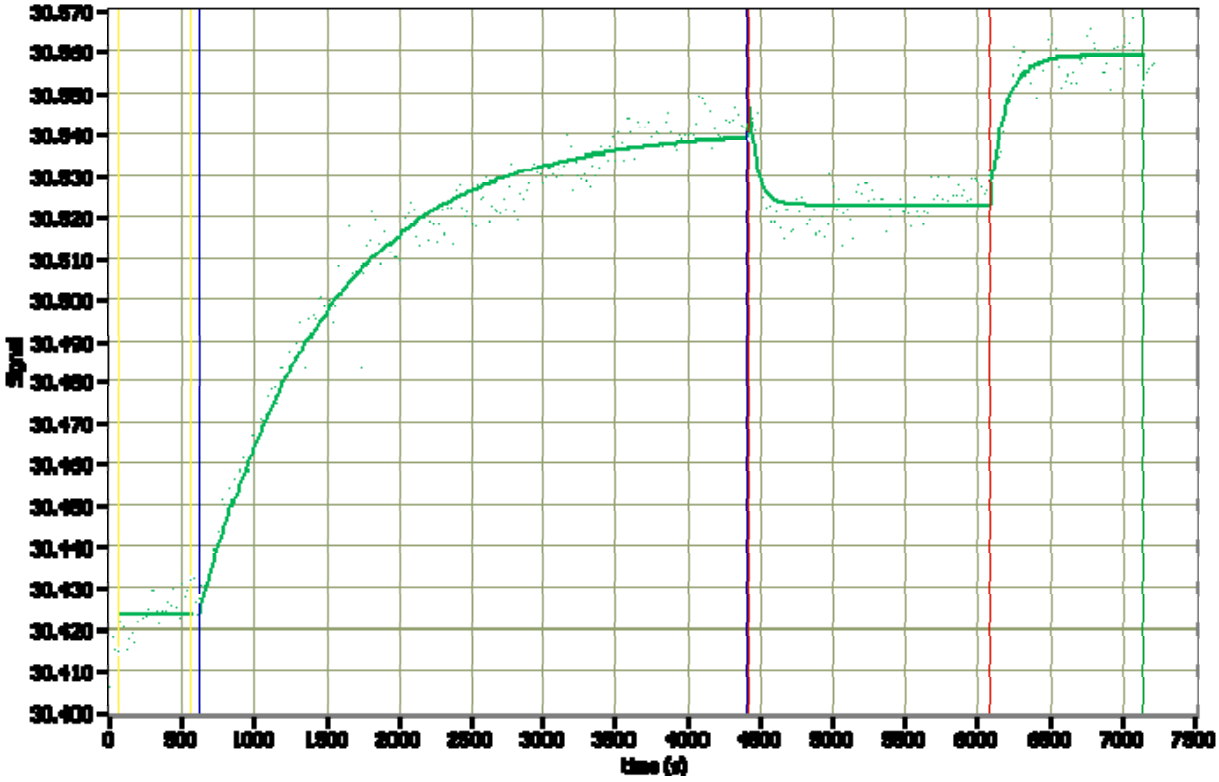

Figure 3-17. Real-time measurement of DMPC bilayer formation on silicon substrate followed by introduction of COM crystals in SPR cell. Ψ signal recorded as a function of time.

Table 3-3. Estimated kinetic parameters values for the fitted experimental data to model for POPC vesicle fusion onto ODM in SPR cell.

Solution (mg/mL)	Tangential constant τ (s)	Adsorption rate constant *kon* ($s^{-1}.M^{-1}$)	Desorption rate constant *koff* (s^{-1})	Equilibrium constant K_D (M^{-1})
POPC 0.75 mg/mL	743.28	4.61×10^{-4}	1.02×10^{-3}	2.17

.

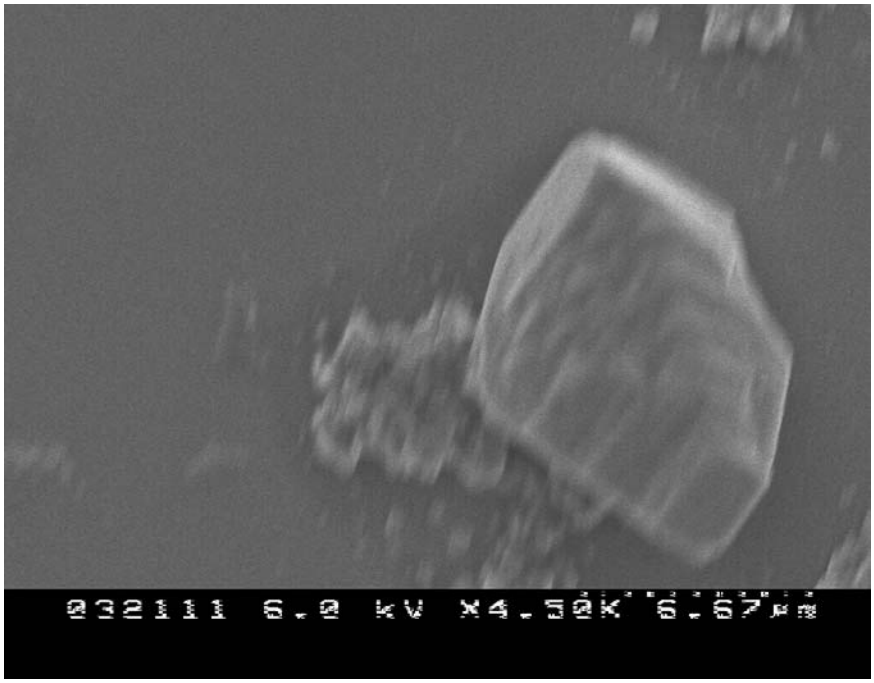

A

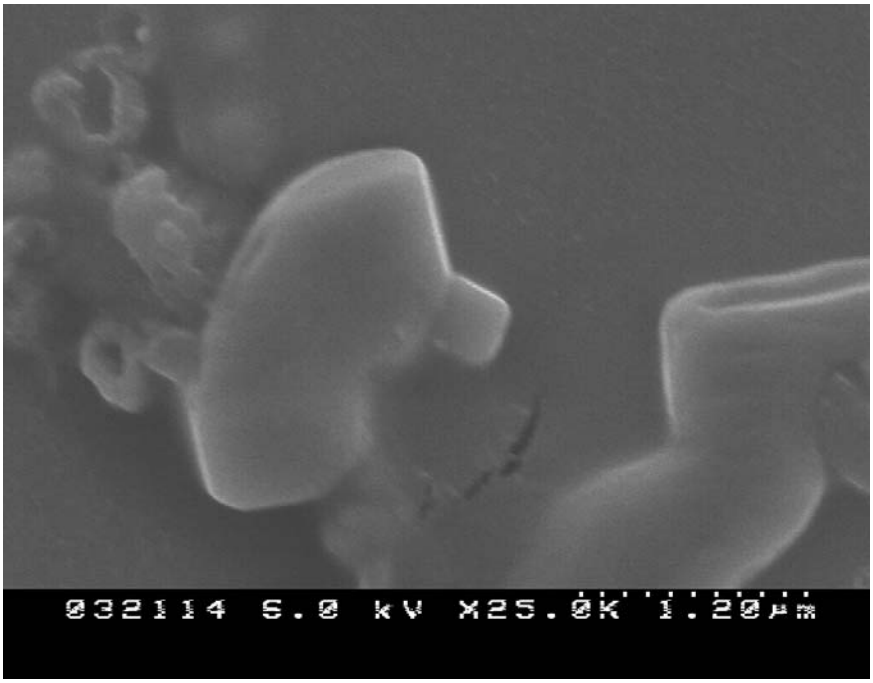

B

Figure 3-18. SEM images of gold and silicon surface after the drying procedure. A) Plate-like crystals characteristic of the morphology of COM crystal on a stone surface. Plate-like angles are close to 120˚. B) COM crystal surrounded by NaCl crystals and Triz HCl crystals.

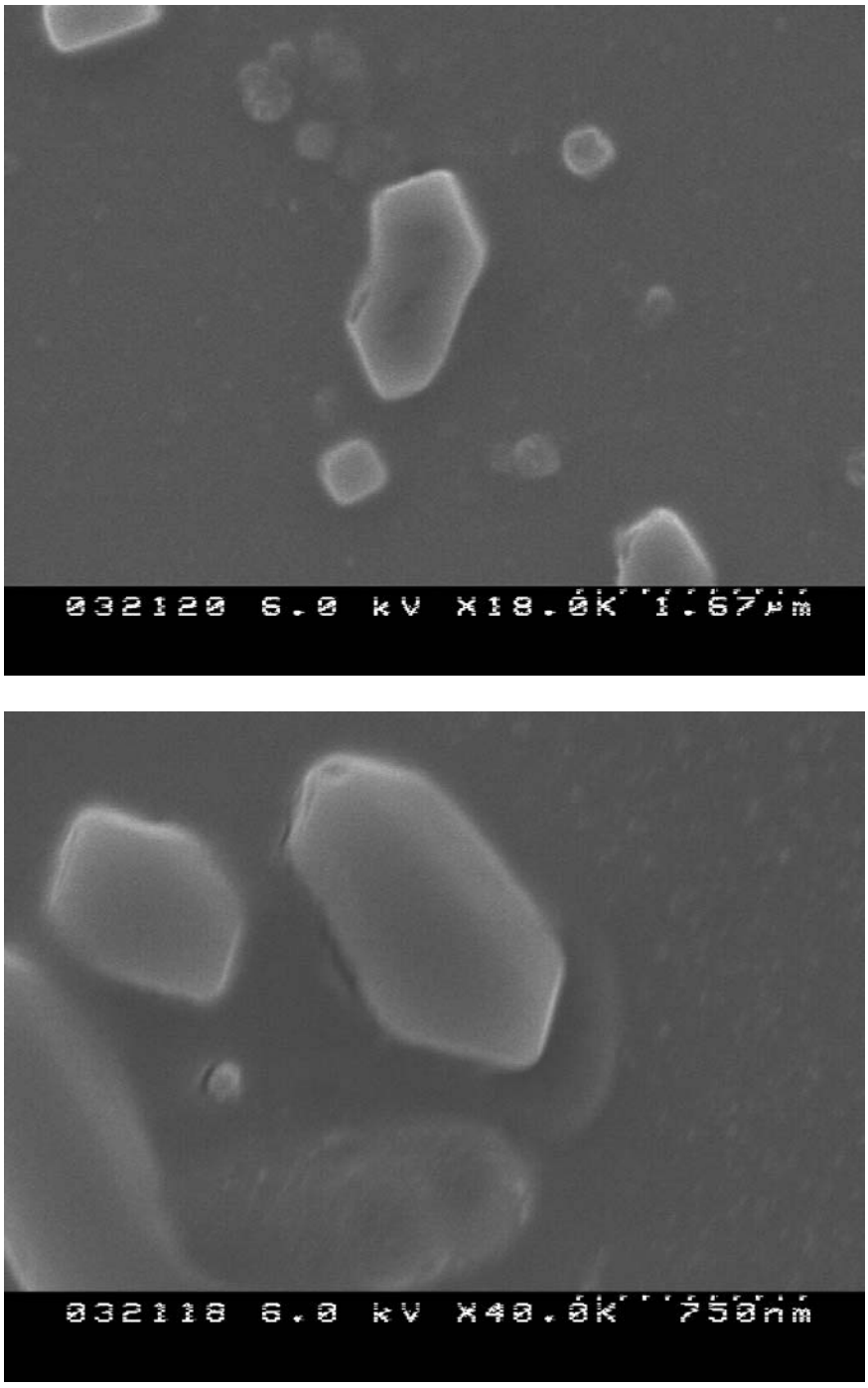

Figure 3-19. SEM images of COM crystals surrounded by NaCl and Triz HCl crystals after the drying procedure. (100) face is normal to microscope view.

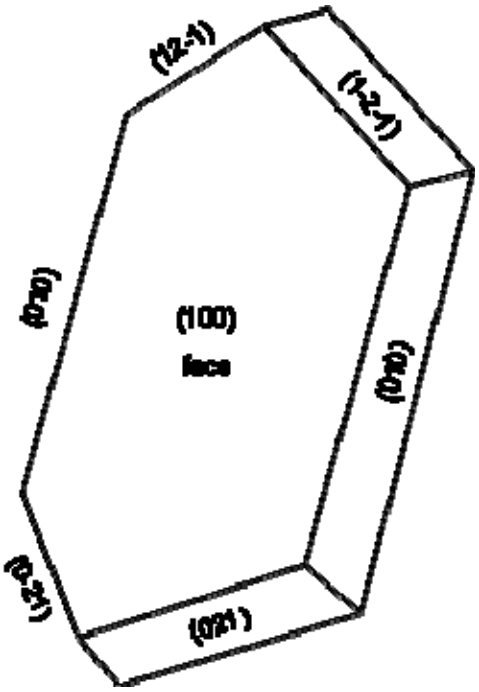

Figure 3-20. Calcium oxalate monohydrate morphology showing prominent facets indexed according to Tazzoli and Domeneghetti [22]

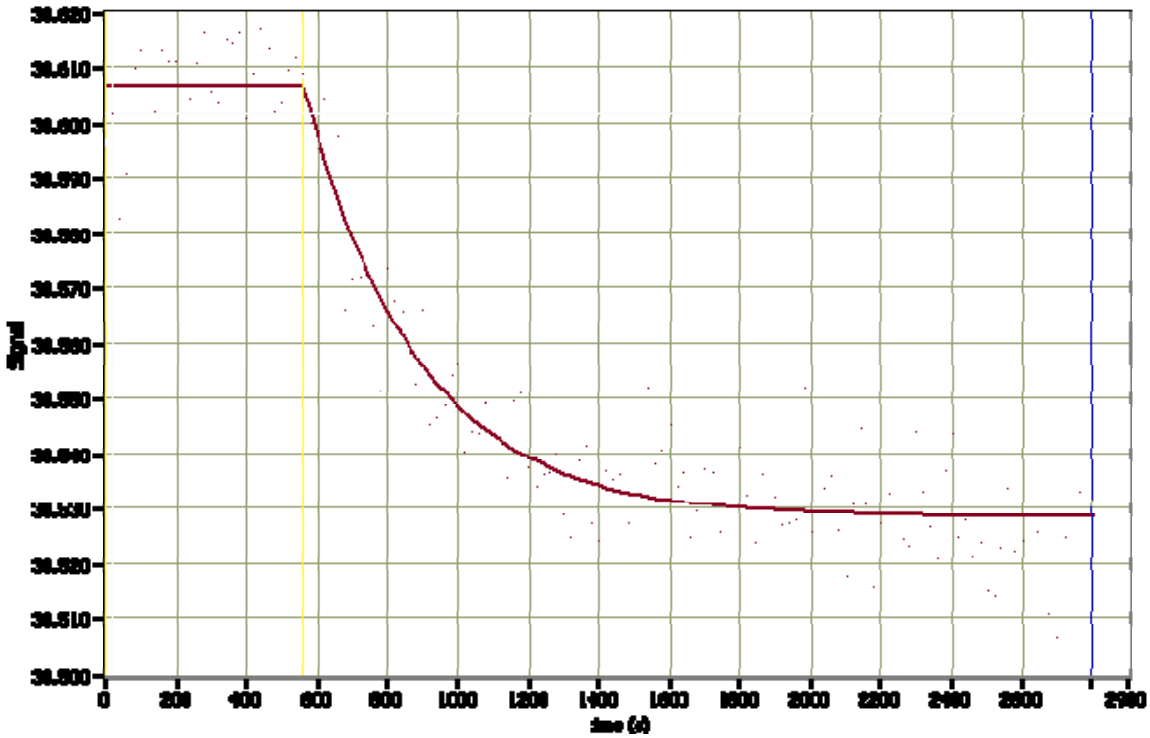

Figure 3-21. Real-time measurement of introduction of COM crystals in solution on ODM self-assembled monolayer. Ψ signal recorded as a function of time with SPR cell.

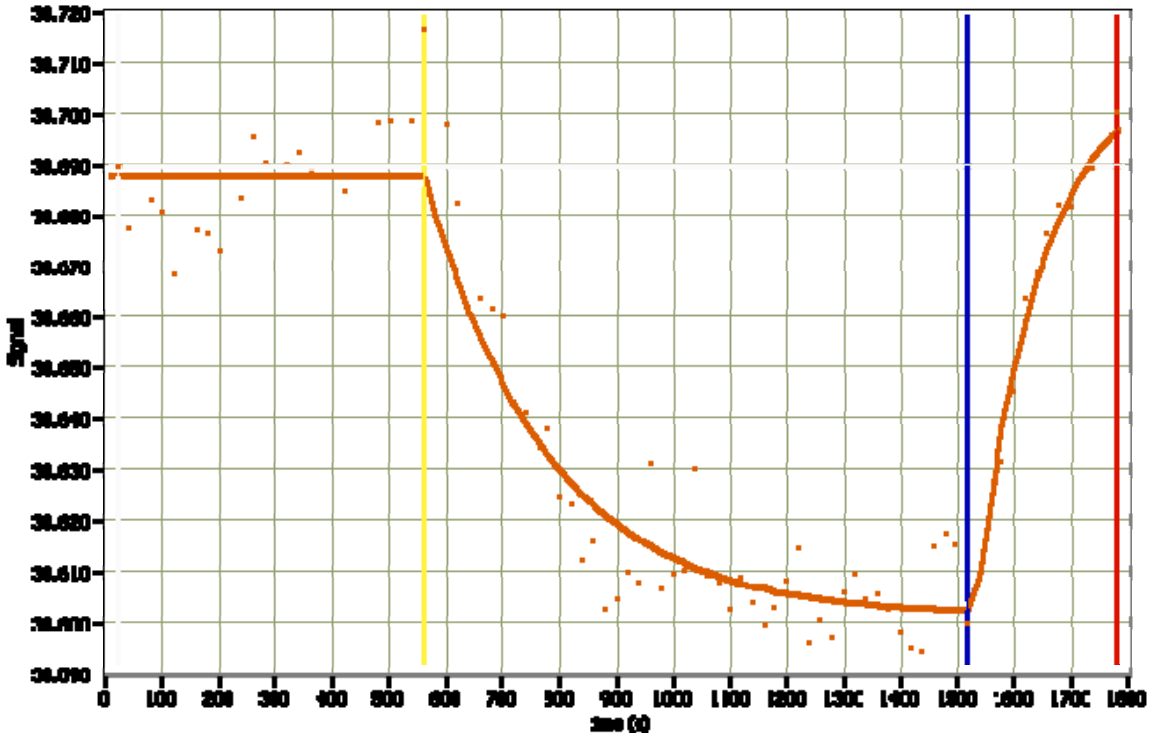

Figure 3-22. Real-time measurement of introduction of COM crystals in solution on gold. Ψ signal recorded as a function of time with SPR cell.

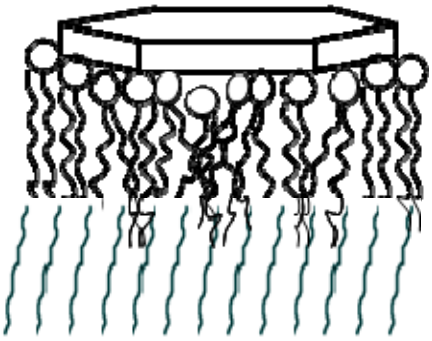

Figure 3-23. Schematic of the possible interaction of COM crystal with a phospholipid monolayer.

Table 3-4. Change in ellipsometric signal when introducing COM crystals onto phospholipid bilayer and monolayer in SPR experiment.

	Ellipsometry experiment in Solid-Liquid cell BILAYER	SPR enhanced ellipsometry experiment MONOLAYER
POPC	32.9%	63.6%

CHAPTER 4
CONCLUSION

As a result of this study, a solid-liquid cell adapted to the EP^3-SW ellipsometer has been designed and fabricated. This solid-liquid cell has been proved to be suitable for solid-liquid interface studies. Through this cell, it has been proved that we can realize Real-time measurements of the deposition of phospholipid bilayers. Imaging ellipsometry can also be used with the SL cell in order to map a surface by derivation of a spatially resolved map of ellipsometric angle, Δ, at a macroscopic scale.

In fact, in this study two methods have been employed to characterize the surface coverage, lateral uniformity and thickness of mono- and bilayer: imaging ellipsometry and kinetic analysis. Imaging ellipsometry with solid-liquid cell enabled noncontact measurements, large-area imaging with high sensitivity to small relative differences in optical properties, real-time measurements and modest spatial resolution. Also important to note, to the use of the solid-liquid cell can be extended to other surfaces –bound configurations of biomaterials, cells, and proteins. Kinetic analysis was also used in this study to monitor the formation of supported phospholipid membranes by vesicle fusion. The kinetics of the process was investigated at different concentrations of a phospholipid. However the vesicle fusion mechanism can be described with more elaborate models. The advantage of using self-assembled membranes as a substrate is that their structure and composition can be determined in-situ by ellipsometry prior to the introduction of COM crystals in solution.

Ellipsometry and SPR enhanced ellipsometry methods are suitable for structure determination in systems that exhibit no lateral ordering in the interfacial plane, as is typical of biological membranes, and can be employed at buried interfaces. Ellipsometry and SPR enhanced ellipsometry were both used to characterize the interaction of COM crystals on

phospholipids. Both methods represent a new way of studying the crystal-lipid interaction never reported before in ellipsometry. SPR enhanced ellipsometry allowed to avoid scattering effect of crystalline solution and support the idea that COM crystals adhere onto membranes and that phospholipid monolayer stability depends on the compositional change of the lipid. The combination of these two analytical methods suggests a new means to observe the adhesion of COM crystals to lipid membranes. The effect of phospholipid composition on the nature of the interaction can be quantitatively characterized by the desorption rate constant and percent of mass change on the lipid interface. The striking difference in the extent of the interaction between DMPC and POPC suggested that chemical difference from the adhesion lies in the hydrophobicity and packing density of the lipid chains. Saturated fatty acids are known to make condensed phospholipid membranes more rigid, whereas unsaturated fatty acids have a negligible effect.

This means that further investigation can be carried out with different varieties of lipids by ellipsometry and SPR enhanced ellipsometry. It also suggests a new mechanism considering the detachment of lipids from the surface and might give more information about the composition of the organic phase of kidney stones and the interaction of kidney stones with cell membranes.

LIST OF REFERENCES

1. Mandel, N. *J. Am. Soc. Neph.* **1994**, *5*, S 37.

2. Verkolen, C. F.; van der Boom, B. G.; Houtsmuller, A. B.; Schroder, F. H.; Romijn, J. C. *Am. J. Physiol.* **1998**, *274*, F958.

3. Bigelow, M. W.; Wiessner. J. H.; Kleinman, J. G.; Mandel, N. S. *Am. J. Physiol.* **1997**, *272*, F55-F62.

4. Lieske, J. C.; Huang, R.; Toback, F. G. *Am. J. Physiol.* **2000**, *208*, F130-F137.

5. Sheng X.; Jung, T.; Wesson, J. A.; Ward, M. D. *PNAS* **2005**, *102*, 267-272.

6. Sandersius, S.; Rez, P. *Urol. Res.* **2007**, *35*, 287-293.

7. Rabinovich, Y. I.; Esayanur, M.; Daosukho, S.; Byer, K. J.; El-Shall H. E.; Khan S. R. *J. Col. Inter. Sc.* **2006**, *300*, 131-140.

8. Talham, D. R.; Backov, R.; Benitez, I. O.; Sharbaugh, D. M.; Whipps, S.; Khan, S. R. *Langmuir* **2006**, *22*, 2450-2456.

9. Azzam, R. M. A.; Bashara, N. M. *Ellipsometry and polarized light. North Holland, Amsterdam.***1977**.

10. Zhdanov, V.; Keller, C.; Glasmaster, K.; Kasemo B. *J. Chem. Phys.* **2000**, *112*, 900.

11. Rossi, C.; Homand, J.; Bauche, C.; Hamdi, H.; Ladant, D.; Chopineau J. *Biochem*. **2003**, *42*, 15273.

12. Werner, K. *J. Electrochem. Soc*. **1990,** *137*, 6.

13. Reimhult, E.; Hook, F.; Kasemo, B. *Langmuir* **2003**, *19*, 1681-1691.

14. Yee, C. K.; Amweg, M. L.; Parick, A. N. *Adv. Mat.* **2004**, *16*, 1184.

15. Plant, A. L. *Langmuir* **1993**, *9*, 2764-2767.

16. Ducharne, D.; Max, J. J.; Salesse, C.; Leblanc, R. M. *J. Phys. Chem.* **1990**, *94*, 1925-1932.

17. Petrov, J. G.; Pfohl, T.; Mohwald, H. *J. Phys. Chem. B.* **1999**, *103*, 3417-3424.

18. Lewis, B. A.; Engelman, D. M. *J. Mol.Biol.* **1983**, *166*, 211-217.

19. Zhdav, V. P.; Keller, C. A.; Glasmastar, K.; Kasemo, B. *J. Chem. Phys.* **2000**, *112*, 900-909.

20. Lingler, S.; Rubinstein, I.; Knoll, W.; Offenhauser, A. *Langmuir* **1997**, *13*, 7085-7091.

21. Williams, L. M.; Evans, S. D.; Flynn, T. M.; Knowles, P. F.; Bushby, R. J.; Boden, N. *Langmuir* **1997**, *13*, 751.

22. Vacklin, H. P.; Tiberg, F.; Giovanna, F.; Thomas, R. K. *Biochem.* **2005**, *44*, 2811-2821.

23. Doherty, W. O. S.; Fellows, C. M.; Gorjian, S.; Senogles, E.; Cheung, W. H. *J. Appl. Poly. Sc.* **2004**, *91*, 2035-2041.

24. Ouyang, J.; Yao, X.; Su, Z.; Cui, F. *Science in China* **2003**, *46*, 3.

25. Khan, S. R.; Glenton, P. A.; Backov, R., Talham, D. R. *Kidney Int.* **2002**, *62*, 2062-2072.

26. Lasis, D. D.; Barenholz, Y. *Hand. Nonmedical Appl. Liposomes: Theor. Bas. Sc.* **1996**, 139.

27. Talham, D. R..; Benitez, I. O. *Abstracts of Papers of the American Chemical Society* **2004**, *228*, U847.

28. Backov, R.; Khan, S. R.; Mingotaud, C.; Byer, K.; Lee, C. M.; Talham, D. R. *Journal of the American Society of Nephrology* **1999**, *10*, S359-S363.

29. Backov, R.; Lee, C. M.; Khan, S. R.; Mingotaud, C.; Fanucci, G. E.; Talham, D. R. *Langmuir* **2000**, *16*, 6013-6019.

30. Whipps, S.; Khan, S. R.; O'Palko, F. J.; Backov, R.; Talham, D. R. *Journal of Crystal Growth* **1998**, *192*, 243-249.

31. Talham, D. R.; Benitez, I. O.; Backov, R.; Khan, S. R. *Abstract of Paper of the American Chemical Society* **2003**, *225*, U51.

32. Letellier, S. R.; Lochhead, M. J.; Campbell, A. A.; Vogel, V. *Biochimica et Biophysica Acta General Subjects* **1998**, *1380*, 31-45.

33. Benitez, I. O.; Talham, D. R. *Journal of the American Chemical Society* **2005**, *127*, 2841-2815.

34. Talham, D. R.; Benitez, I. O.; Sharbaugh, D. M.; Whipps, S.; Khan, S. R. *Langmuir* **2006**, *22*, 2450.

35. Kucerka, N.; Tristram-Nagle, S.; Nagle, J.F. *Biophys. J.* **2006**, *90*, L83-L85.

36. Kucerka, N.; Liu, Y. F.; Chu, N. J.; Petrache, H. I.; Tristram-Nagle, S. T.; Nagle, J. F. *Biophys. J.* **2005**, *88*, 2626-2637.

37. Kucerka, N.;Kislev, M. A.; Balgavy, P. *Eur. Biophys. J. Biophys. Lett.* **2004**, *33*, 328-334.

38. Stroumpoulis, D.; Parra, A.; Tirelli, M. *AIChE Journal* **2006**, *52*, 8.

39. Seu, K. J.; Cambrea, L. R.; Michael Everly, R.; Hovis, J. S. *Biophysical Journal*, **2006**, *91*, 3727-2735.

40. Wang, S. J.; Ong, C. K.; Xu, S. Y.; Chen, P.; Tjiu, W. C.; Huan, A. C. H.; Yoo, W. J.; Lim, J. S.; Feng, W.; Choi, W. K. *Semicond. Sci. Technol.* **2001,** 16, L13-L16.

41. Koenig, B. W.; Strey, H. H.; Gawrisch, K. Biophys. J. 1997, 73, 1954-1966.

BIOGRAPHICAL SKETCH

Anne-Sophie Widede Bouridah was born on July 06, 1984 in Grenoble, France. Her parents are Karim and Marie-Paule Bouridah of The Hague, Netherlands. She attended the Lycee Francais Vincent van Gogh and graduated from a baccalaureate with honors in 2002. Starting fall 2002, she accomplished two years of intensive preparatory class in Math, Physics and Chemistry to enter at the Chemistry and Physics Engineering School of Bordeaux (ENSCPB) in 2004. During her third year of engineering school, she enrolled in the graduate program in the Department of Chemistry at the University of Florida, Gainesville, Florida. Her area of specialization is analytical chemistry, and her research was directed by Dr. Daniel R. Talham. She is now looking forward to implement her knowledge and experience the industrial environment.